Addis Ababa University
Addis Ababa Institute of Technology
School of Graduate Studies
Mechanical and Industrial Engineering
Thermal Engineering

Manufacturing and Experimental Performance Analysis of a Micro Hydro Pelton Turbine

By: Kassa Dejene Legese

A Thesis submitted to the School of Graduate Studies of Addis Ababa University in partial fulfillment of the requirements of the Degree of Masters of Science in Thermal Engineering

Advisor

Dr.-Ing. Edessa Dribsa

Co-Advisor

Ato Tilahun Nigussie

June, 2018

Addis Ababa Institute of Technology
School of Graduate Studies
Mechanical and Industrial Engineering
Thermal Engineering

Manufacturing and Experimental Performance Analysis of a Micro Hydro Pelton Turbine

By: Kassa Dejene Legese

Approved by the Examining Board:

Dr.-Ing. Edessa Dribsa _____

Advisor

Ato Tilahun Nigussie _____

Co-Advisor

Dr. Kamil Dino _____

External Examiner

Dr.--Ing. Wondowssen Bogale _____

Internal Examiner

Dr. Yilma Tadesse _____

Dean, SMiE

Dr. Ermias Tesfaye _____

Assoc. Graduate Program Director

Signed Declaration

I declare that the thesis for the M.Sc. degree at the University of Addis Ababa, hereby submitted by me, is my original work, and has not been previously submitted for a degree at this or any other university, and that all reference materials contained therein have been duly acknowledged.

Name: Kassa Dejene Legese

Signature: _____

Abstract

To ensure sufficient alternative energy for future, considering renewable energy is an idea with no question. Having said this, Ethiopia is a country blessed with different kinds of renewable energy resources. One of the most effective renewable energy in Ethiopia is hydropower, which uses hydraulic turbines to generate electricity.

According to the way of energy transfer, there are two types of hydraulic turbines namely impulse turbines and reaction turbines. From impulse turbine, Pelton turbine has an excellent establishment of micro-hydroelectric power plant, due to its simple construction and ease of manufacturing. However, there is no local company or institute, which manufactures hydro turbines yet. Having this in mind, localization and manufacturing of hydro turbines plays a crucial role economically for the development of the power sector in Ethiopia.

This study aims in manufacturing and performance lab testing analysis of Pelton turbine with specification of Power of 2KW, flow rate of 20.8 Lit/sec, height of 13.3m and Pitch Circle Diameter (PCD) of 212mm, in order to develop a manufacturing manual while helping localize renewable energy technologies in hydropower sector.

SOLIDWORKS and Matlab software, 3D printing, sand casting, lathe machine, welding machine and drilling machines were used to manufacture the turbine according to the design results.

From this study, the manufactured turbine has an overall efficiency of 54.09%, which is 3.41% less from the expected theoretical value at 75% valve opening. Hence, micro hydro Pelton turbine was able to manufacture and then manufacturing manual was developed. Finally, laboratory test results have been evaluated and good agreement between performance curves of simulation and experimental test at designed turbine speed. This shows the manufactured Pelton turbine is effectively fabricated locally and thus the fabrication methodology followed could be used as a manufacturing manual for local developers. The variation between theoretical and experimental test result and simulation with experimental test result was occurred due to quality of manufacturing (especially casting of bucket) and inconvenience test rig at AAiT.

Key words:-Small Hydro Power, Micro Hydro Pelton turbine, Efficiency, Manufacturing, Manual.

Acknowledgment

I would like to thank my advisor Dr.-Ing. Edessa Dribsa and Co-advisor Ato Tilahun Nigussie for their priceless support, feedback, and encouragement. And also, I am deeply grateful to my lovely family especially to my wife Engineer Seblewongel Tesfu and my two kids Gabriela and Nolawi Kassa and all of my friends especially Ato Hiluf Getahun for their everlasting support throughout this thesis work especially.

Table of Contents

List of Tables

List of Figures

Nomenclature

Q	Volume flow rate
H_i	Inlet Head
P_h	Hydraulic Power
P	Power
N	Speed
RPM	Revolution Per Minute
T	Torque
p	Pressure in Pascal
P_{in}	In put hydraulic power supplied by the water,
Q_u	Unit flow rate
Qdesign	Designed flow rate
N_u	Unit speed
P_u	Unit power
P_w	Power out
Fw	Force produced on the bucket
R_w	wheel radius
$\dot{m}$	mass flow rate [kg/s]
W1	Relative flow velocity at bucket entry
C_1	Jet speed at nozzle exit
Co	Jet speed
U	Peripheral speed
g	Acceleration due to gravity 9.81m/s^2
C_2	exit velocity at bucket
W	Relative flow velocity
Ws	Weight of spring balance

Greek symbols

η_o	Overall Turbine Efficiency
η_m	mechanical efficiency
η_h	Hydraulic efficiency
η_t	Theoretical Efficiency
η_{design}	Designed Turbine Efficiency
ω	speed in r ad per sec
κ	ratio of bucket speed to jet speed
β_2	Bucket exit angle

Abbreviations

AAiT	Addis Ababa Institute of Technology
FDRE	Federal Democratic Republic of Ethiopia
MoST	Ministry of Science and Technology
MHP	Micro Hydro Power
PCD	Pitch Circle Diameter

Chapter One

Introduction

This chapter deals with an overview of the Manufacturing and Testing of Micro Hydro Turbine where it consists of the research background, problem statement and its objectives. Furthermore, the methodology and thesis organization will be discussed.

1.1 Background of the Study

Big effort has been taken by the government of Ethiopia in generating power nowadays and reaches 400MW generating capacity per year [1] although grid coverage for remote areas is not expected to be fulfilled in near future as it currently reaches only 55% [1]. Thus off grid power sources play vital role to provide electricity for remote villages in the country.

Industries, mega cities, towns, and export market shall consume the national power supply coverage, which generates power from mega projects. However, for rural areas that have a renewable energy potential like small hydropower can generate power to self-sustain and again can tot up the national grid in its excess power.

There are rivers flowing throughout the year in Ethiopia with reasonable head and flow rate. The potential of small hydro of the nation is expected to be 1500MW to 3000MW [2], which are enormous. Consequently, exploitation of small hydro potential in remote areas installing small hydro plants could be the best option as they can be environmentally friendly as well as cost effective. As a result, local power generation equipment manufacturing becomes critical in alleviating the nation thereby boosting national growth.

Manufacturing of Pelton turbine in the world is very well known and there are global leading manufacturers like ANDRTIZ, INSET Ltd, WATERGENPOWER, IREMSPA, GLIKES and many others but at micro scale in Africa, there is limited usage of this turbine even if there is a limited trial.

In Rwanda, a 10 KW micro Pelton turbine was manufactured and installed but the turbine buckets were fabricated in UK [7].

In South Africa 88KW capacity Pelton turbine were fabricated locally and tested in 2017 that implies localization of micro turbines is emerging in Africa [17].

In Nigeria 668W Pelton Turbine were designed, constructed and tested at UNILORIN dam with 4m head in 2014. Again, in the same year, a German based company called Smart Hydro Power Ltd. supplied thirteen turbines. Still in Nigeria, the turbines are imported [24].

In Kenya V*ery small hydropower (*pico hydro) schemes, with an output of less than 5kW, can be a cost-effective option for the electrification of remote rural communities. In order to achieve low installation cost per unit power output, and hence low energy costs, it is necessary to select the components of the scheme to reduce cost and increase efficiency [26].

At large scale Ethiopia has the experience in installing of Pelton Turbine at Gilgel Gibe2 hydro power plant, but at small scale the country has no experience in this turbine even though Ethiopia have number of small rivers that have a potential to generate micro and small scale power. The existing experience in micro scale power generation was using cross flow turbines. These turbines were supplied by Ethiopian Rural Energy Development & Promotion Centre from abroad with hard currency and some are manufactured and installed by GTZ and Selam Technical College [2].

Considering topography for many small-hydro sites existing in Ethiopia, a Micro Hydro Pelton turbine can be a best option as most of our rivers are flowing from higher altitudes keeping in mind 70% mountains in Africa are found in Ethiopia [27] and the nation is thus blessed with high head. These turbines have advantage of producing a lot of power from a small unit at high head. In addition, they are reasonably easy to manufacture. Nonetheless, up to date there is no company or institution engaged in supplying small Micro Hydro Pelton turbine in Ethiopia.

1.1.1 Overview of Local Manufacturing of Micro Hydro Turbines

Ethiopia is blessed with renewable energy resources like hydro, which up to now generated only about 4120MW within a long history of power generation, which is nearly 9% of its potential [1]. Estimation of the economically feasible potential for hydropower in Ethiopia is expected to be 45,000 MW [1].

The landscape of Ethiopia is well suited to the use of micro-hydro power. There are mountainous areas with many small rivers that are convenient for development of small and micro-hydro power generation. Nevertheless, the extent of micro-hydro power (MHP) development is very limited in Ethiopia although the technology has been in practice since the last century. There is a long history of using waterpower, as traditional "Arab axis mills" have been in use in some areas for over a hundred years [2].

There were over a dozen of MHP schemes in Ethiopia. Much of them are not functional [4]. Today, there are only three MHP schemes functional with a cumulative installed capacity of 6.15 MW in the country [2].

Although there were long history of micro-hydro power (MHP) in Ethiopia, the adaptation of modern MHP technologies is not very well integrated and local technical skills are not well developed. At the moment, in spite of the fact that MHP is known to Ethiopia for so long specifically for water wheels and cross flow turbines, MHP equipment and components are not available off-the-shelf in the local market as there is no institution or company engaged in manufacturing of hydro turbines yet.

Thus, in this study it is tried to fill the gap by manufacturing of Micro Pelton Turbine and thereby localization of the technology will be initiated and will play an icebreaker role in the development of indigenous knowledge and skill by technology transfer to enable the nation to build its generation plants by local capacity.

1.1.2 Theoretical Background of Pelton Turbine

Pelton Turbine is a hydraulic ‘impulse’ turbine, in which water jets hit ‘buckets’ on a wheel as shown in Figure 1.1. The force produced by the jet impact at right angles to the buckets generates a torque that causes the wheel to rotate, thus producing power [16].

The Pelton Wheel needs a source of water in order to run. If the head of water is known, along with the flow rate, then it is possible to find the best size of wheel to use, how fast it should rotate to obtain the maximum efficiency, and what power it is likely to develop.

The velocity in the jet can be estimated by using the known fixed head described as in Equation 1.1. The diameter of the jet can then be found from the known flow rate. A suitable wheel

diameter can be chosen in relation to the jet size. The best speed of rotation may then be selected, such that the speed of the buckets is approximately half that of the jet speed.

$$C_o = \sqrt{2gH} \quad \text{----------1.1}$$

Where: C_o – Jet speed

H –The net pressure head at the inlet of injector

g –Gravity

The power delivered in the jet can be calculated from the speed and cross-sectional area of the jet. The power developed by the Pelton wheel will be less than this, in the ratio of the wheel's efficiency, which may be estimated by reference to the known performance of existing machines of comparable size and output.

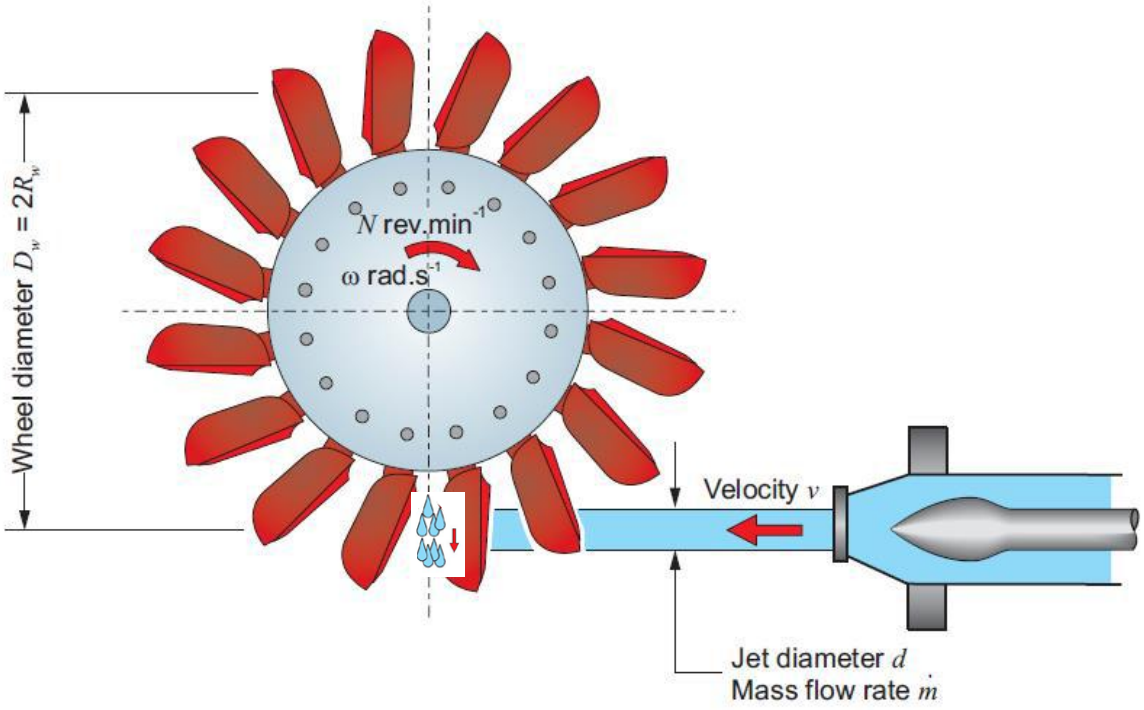

Figure 1.1: Pelton wheel lay out (BURSA, 2016)

The Pelton wheel is usually chosen when the available head is high, but the flow rate is comparatively low [28].

A) Force Exerted by a Jet

Figure 1.2 shows a water jet emerging at speed Co from a nozzle, and striking one of the buckets of the wheel, which itself is moving at speed U. The mass flow rate is and it is assumed that all of the water emerging from the nozzle strikes one or other of the set of buckets arranged around the periphery of the wheel, although, for simplicity, just one bucket is shown in the diagram.

The interaction between the water jet and the bucket is considered directly in the relative moving system. For the flow at the bucket entry and with$C_1 = C_0$, the relative velocity between the jet and moving bucket is given by:

$$W_1 = C_1 - U \quad \text{---------- 1.2}$$

Where:W_1 −Relative flow velocityat bucket entry

C_1 −Jet speed at nozzle exit

U −Peripheral speed

With this relative velocity, the jet flow spreads in the bucket, forming a water sheet. The change in the direction of the flow along the bucket surface is coupled with a pressure increase below the water sheet as related to the impulsive force and determined by the law of momentum. On the surface of the water sheet where the atmospheric pressure is constant, the flow velocity is equal to W_1provided that frictionless flow is assumed.

Once the water flow reaches and then leaves the bucket exit at an angle β, it is again subjected to atmospheric pressure. The relative velocity of the total water flow is then reset to its initial value according to Equation (1.2).

The absolute velocity is thus given by:

$$C_2{}^2 = U^2 + W^2 + 2UW \quad \text{----------} -1.3$$

Where:C_2 −exit velocity at bucket

W − Relative flow velocity

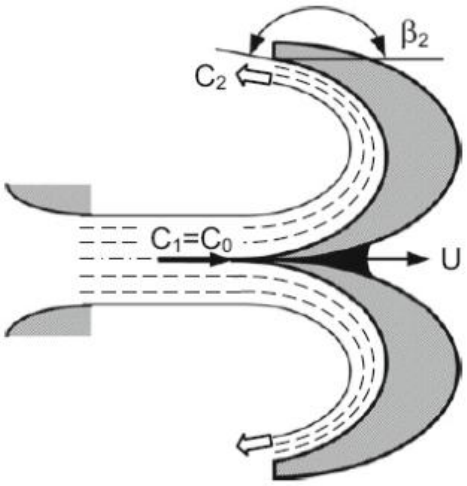

Figure 1.2: Water jet striking bucket (Zh. Zhang, 2016)

According to the balance law of momentum, the change of the flow direction is always related to an external impulsive force which acts perpendicular to the flow direction. This force is nothing else than the pressure below the water sheet. For its determination, the momentum flux difference between the entry and the exit of the moving bucket must be evaluated. The component of the total force in the direction of the bucket motion is calculated by the following momentum balance equation: [16].

$$F_{bucket} = \dot{m}_w W(1 - \cos\beta_2) \quad \text{---------- 1.4}$$

Where: $\dot{m}_w$ −Mass flow in the rotating system

β_2 −Bucket exit angle

It is helpful to express the ratio of bucket speed U to jet speed Co as k:

$$k = \frac{U}{Co} \quad \text{---------- 1..5}$$

So that

$$\mathrm{F}_{bucket} = \dot{m}_w \mathrm{Co}(1 - k)(1 - \cos\beta_2) \quad \text{---------- 1.6}$$

B) Torque Exerted on the Wheel

$$T_{max} = \dot{m}_w R_w Co(1 - k)(1 - \cos\beta_2)$$

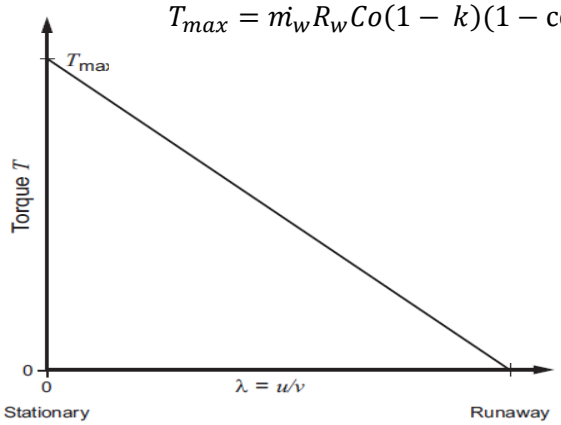

Remark* **λ=u/V *is substituted by* **k=U/Co** *for this paper*

Figure 1.3: Variation of torque T with speed ratio λ (BURSA, 2016)

The torque T exerted on the wheel is described as:

$$\mathrm{T} = \dot{m}_w R_w \mathrm{Co}(1 - k)(1 - \cos\beta_2) \quad -----1.5$$

Where: k −speed ratio

Co −Jet speed

R_w −Wheel radius

We see that for a particular wheel, supplied with water at some fixed flow rate (so that both ṁ andCo are also fixed), torque T varies as (1 – k). The torque therefore falls linearly from a maximum when k = 0 (i.e. when the wheel is stationary) to zero when k = 1 (i.e. when the bucket moves at the same speed as the jet). This is referred to as the runaway condition. In Figure 1.3 the expected Torque Vs Speed curve is shown and was used in comparing the experimental results.

C) Power Output

The power output P_w developed at the wheel is given below by:

$$P_w = \omega \mathrm{T} \quad -----1.6$$

Where:ω- is speed in rad per sec

And noting that:

$$T = \omega R_w \quad -----1.7$$

The power output $P_w$may be written as:

$$P_w = \dot{m}_w \mathrm{Co}^2 k(1-k)(1-\cos\beta_2) \quad -----1.8$$

D) Hydraulic Efficiency

The power input P_{in}, in the form of kinetic energy in the jet, is:

$$P_{in} = \frac{1}{2}\dot{m}_w \mathrm{Co}^2 \quad -----1.9$$

Without an accurate figure for the jet diameter, the inlet pressure (shown on a small gauge) and water flow (measured by the hydraulic bench) gives a good approximation of the inlet power from:

$$P_{in} = Q_\upsilon p \quad ----- 1.10$$

Where Q_υ is in $m^3.s^{-1}$ and p the pressure is in Pascal.

The hydraulic efficiency η_{hy}, defined as the ratio of output power to input power is:

$$\eta_h = \frac{P_w}{P_{in}} = 2k(1-k)(1-\cos\beta_2) \quad -----1.11$$

With a maximum value:

$$\eta_{max} = \frac{1}{2}(1-\cos\beta_2) \quad -----1.12$$

In terms of percentage:

$$\eta_h = \frac{P_w}{P_{in}} \times 100\% \quad -----1.13$$

It must be emphasised that the hydraulic efficiency used here gives the ratio of hydraulic power generated by the wheel to the power in the jet. The overall efficiency of the turbine will fall short of this hydraulic efficiency due to some loss of head in the nozzle, air resistance to the rotating turbine, and losses at the bearings.

The efficiency of small, locally manufactured Pelton turbines is normally not as high as with larger turbines. It is therefore, recommended to calculate the turbine parameters with an efficiency of 0.70 to 0.85. This may result in an efficiency of 0.5 to 0.6. Figure 1.4 represents Power versus speed curve of a Pelton turbine [25].

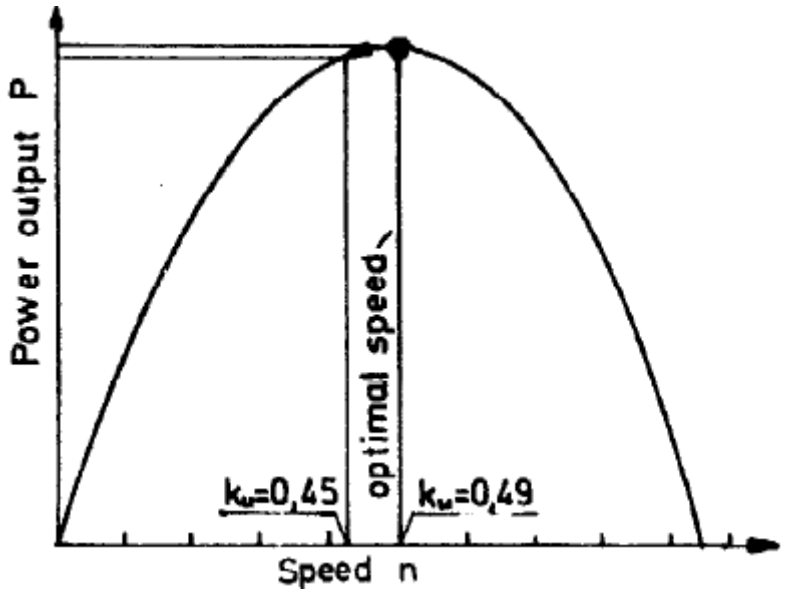

Figure 1.4: Power versus speed curve of a Pelton turbine. [Markes Eisenring, 1991]

1.2 Statement of the Problem

Even if some small river's topography of Ethiopia are very ideal in generation of micro/small hydro power and even mega power by cascading turbines using Pelton turbines, which are ideal turbines for high head (majority of Ethiopian small rivers have high head) and low flow rate, there is no institution that fabricates and installs this turbines locally yet.

The purpose of this study is to manufacture and test model Pelton turbine. This gives technical skill which in-turn build a national confidence in constructing generation plants using local capacity possibilities while the documentation serves as a manual for local manufacturers.

1.3 Objectives of the Thesis

The objective of this thesis is to manufacture and determine experimentally the performance characteristics of the Micro hydro Pelton turbine designed and optimized by PhD candidate Ato Tilahun Nigussie.

As a result, this thesis has the following specific objectives

- Preparing manufacturing drawing of the designed Micro hydro Pelton turbine components,
- Manufacturing Micro hydro Pelton turbine parts,
- Testing manufactured turbine and
- Preparing a manufacturing manual.

1.4 Methodology

The methodology held here is developing manufacturing drawings using Solidworks, manufacture Pelton turbine locally and then validate experimental result with theoretical and simulated results done by Ato Tilahun Nigussie using excel spreadsheet.

1.4.1 Data Collection

Optimized bucket and other turbine parts design done by Ato Tilahun Nigussiewas taken as an input for the manufacturing of Pelton turbine. Then manufacturing drawings were prepared, materials to be used for manufacturing the turbine were identified and prior to the development of the methodology, a survey is conducted on selection of workshops in AAiT and Private Institutions.

1.4.2 Analysis

To accomplish the desired objectives, literature review both on hydraulic machinery theory and on the manufacturing /machining and casting manuals and other resources that were relevant to this thesis work followed. SOLIDWORKS software was used to obtain manufacturing drawings. SOLIDWORKS is a computer aided design and computer-aided engineering computer program which is used for solid modeling published by Dassault Systems.

Excel spreadsheet were used to analyze experimental data. It is used to validate the experimental result considering different inputs(flow rate, head, and speed) and output values (power, torque, efficiency).

3D printing, sand casting, lathe machine, welding machine and drilling machines were used to manufacture the turbine according to the design results.

1.5 Thesis Organization

This thesis work as shown in the following has six chapters:

The first chapter discusses the general overview of the manufacturing of Pelton turbine. Introduction, background, statement of the problem, objective of the study and methodology are also presented in this chapter.

Chapter two is a literature review part. In this chapter different literature related to Manufacturing and testing of micro Pelton Turbine are briefly discussed.

Chapter Three illustrates the Manufacturing of the turbine. Preparation of manufacturing drawing using SOLIDWORS, both 3D and 2D drawing, pattern development for the runner buckets, casting procedures of buckets, fabrication of other turbine components and assembling of turbine are discussed.

Chapter-four illustrates the Testing of the Pelton turbine. Testing procedures, test bench modification, testing of the performance of the turbine test, data collection and calculations based on the data collected has been discussed.

Chapter-five summarizes the results obtained. Using the test data and calculated data, efficiency of the turbine are achieved and turbine characteristic curves from the test result are compared with theoretical results. Conclusions and Recommendations are presented in this chapter too.

Chapter Two

Review Literature

For a country that intends to lead its economy by industry and to become a middle level economic country by 2020, exploiting its generation potential including pico, micro and small levels utmost is critical and will play a pivotal role in achieving it.

Previous research on Pelton turbines consist mainly of analytical, numerical and experimental studies. In this present work, reviews on experimental studies of micro Pelton turbine were carried out through local manufacturing and testing of the Pelton turbine in AAiT's Hydraulics Laboratory.

E. Quinox successfully designed fabricated and constructed a 10KW Micro hydro Pelton turbine in 2013 [7] in Rwanda. The organization uses Pelton cups or buckets manufactured in UK but in this study all parts of the turbine are manufactured locally except other mechanical parts like bearings with housings, belts, o-rings bolts and nuts with washers.

William Bolon, Vasu Sharma, Manjot Singh designed, manufactured and tested a Pelton turbine with an epoxy resin made buckets in 16 March, 2010 [3] and uses balsawood for their pattern development which is much inaccurate than 3D printing pattern development technique using ABS-P430 thermoplastic material[5].

Vesely, et.al conducted the upgrading of a 62.5 MW Pelton turbine by refurbishing the runner and nozzles. The rated capacity increased by 9% and efficiency increased by 1.4%. Heinz et.al [10] carried experiment to estimate the influence of splashing water distribution in turbine casing. They showed that the casing has a great influence to the operation of Pelton turbines and so it is very important to include casings as important factor in all investigations.

A Group of staff in University of Technology, Republic of Iraq, has prepared a laboratory manual for fluid machineries with a title "Scrip of Fluid Machinery" in 2014[12] particularly the paper describes 4 type of experiments for Pelton Turbines to evaluate the performance of it.

AudriusŽidonis, George A. Aggidis performed an experiment to determine optimum number of buckets .The experimental testing was performed at the Laboratory of Hydraulic Turbo Machines of National Technical University of Athens. The laboratory test rig and the measuring

procedure complied with the international model test standards IEC 60193:1999 [14].Finally, comparing the experimental results to the numerically predicted and analyzing the interference between the jets the main limitation of simplified CFD model was identified.2015

Marcus Eisenring in its Volume 9 describes the design, local manufacturing and testing procedures. More emphasis is given to balancing of the turbine particularly for local manufacturers and static balancing is recommending for micro turbines [16].

L K Gudukeya and C Mbohwa studies and compares current fabrication processes and other processes such as laser and electron beam cutting and welding, pressure die casting, investment casting and milling. These processes and use of stainless steel resulted in the least rough finish. This gave an overall increase of 20 – 25% on the turbine efficiencies [17].

Mina Takagi1, Yoshinobu Watanabe, Shinya Ikematsu, Takayoshi Hayashi, TokihikoFujimoto and Yukihiro Shimatani designed Pelton buckets to fabricate via 3D printer. They compare the power generation capacity with one purchased from New Zealand to investigate its effectiveness and efficiency. In their results of the experiment, the power generation curves for each turbine are approximately equal. The power increases continuously with increases in the flow rate. The maximum power generated by each turbine is approximately the same [18].

Williams S Ebhota1 , Akhil S Karun2 and Freddie L Inambao1 studied in improving the surface properties of a Pelton turbine bucket via centrifugal casting technique using model test standard, COMESA 284 (2007) (English/French): Hydraulic turbines, storage pumps and pump turbines Model acceptance tests [15]. This COMESA standard is technically identical to IEC 60193:1999, Hydraulic turbines, storage pumps and pump-turbines.

Saif Aldeen Saad Obayes and **Mohammed Abdul Khaliq Qasim** [19] investigated experimentally the effect of different nozzles, water head and discharge on the performance of Pelton turbine system. The effect of five different nozzles with outlet diameters of (3.61, 5.19, 8.87, 12, and 14.8) mm has been studied. The tip and hub diameter of the Pelton wheel of (269.89, 221.29) mm has been used with different nozzles. The result showed that when increasing in nozzle diameter lead to increasing the discharge and reduction water head.

Lorentz Fjellanger Barstad[20] developed and validated a CFD model that predicts the torque applied to a non-stationary Pelton bucket, subject to a high-speed water jet. Numerous simulations were conducted, testing mesh dependency and different operational points (e.g. head). A comparison of the numerical and experimental measurements showed that the CFD model over-predicts the torque by approximately 1.5%. The result suggests that the numerical model is promising as a parametric design tool, but further development is required to obtain a true validation of the model.

Y.BEUCHER, E. BOULAWZ KSAYER, D. CLODIC [21] in this journal a Pelton wheel has been realized with aluminum buckets and has been mounted on a test bench. The examination of experiments dealing with drag force in the Pelton turbine shows that the wheel friction losses are an important part of turbine losses when it shrouded and operate in high-density atmosphere.A CFD model of Pelton wheel has been done to analyse and reduce the friction losses in order to develop an efficient turbine. Modelling shows that with lowering the number and the size of the buckets, friction loss can be decreased by 30%.

Chukwuneke J. L. Achebe C. H. Okolie P. C. Okwudibe H. A.[22] Chukwuneke J. L.[22] investigated through experiment the effect of head and bucket splitter angle on the power output of a pelton turbine (water turbine), to improve the power generation by the use of efficient Hydro-electric power generation systems. Experiments were conducted on pelton turbine head conditions, high head and low flow within creased pressure delivered more energy on the bucket splitter, which then generates a force in driving the wheel compared to the result obtained from low head and high flow operating conditions. The force generated by the bucket was increased (0 to 0.38N) due to the energy delivered to the wheel by the head, the turbine output increases from (0 to 7.47kW) which influences the output. This increase in the power output was as a result of their head conditions and the bucket splitter angle.

Bryan R. Cobb, Kendra V. Sharp [23] a laboratory-scale test fixture was constructed to test the operating performance characteristics of impulse turbines. Tests were carried out to determine the effect on turbine efficiency of variations in speed ratio and jet misalignment on two Turgo turbines. The results were compared to similar tests in the same fixture on a Pelton turbine. Under the best conditions, the Turgo turbine efficiency was observed to be over 80% at a speed ratio of approximately 0.46, which is quite good for pico-hydro-scale turbines. The results stress

the importance of proper system design and installation, and increase the knowledge base regarding Turgo turbine performance that can lead to better practical implementation in pico-hydro systems.

NYAGROWA MIMISA DICKENS [25] at Jomo Kenyatta University of Agriculture and Technology studied the variance of the power output and overall efficiency against discharge with the head retained as a constant at normal speed. Other parameters necessary for the study were also measured and recorded for the study. The pelton wheel under study was of a smaller scale though it acted as a representative of a similar system in large scale. This experiment was carried out with an acceptable level of accuracy.

Vijaya Bijukchhe[26] at University of Iowa performed a CFD simulation of the 8-inch model axial turbine using simulation software ANSYS CFX to develop the performance curve and determine the turbine efficiency at working load condition. Five simulations were run with the data from the experiment for 30 feet of head across the runner. With the plot of RPM vs. power, it was observed that the power developed at the optimum point was matching with the power generated from the experiment whereas for the overload condition it was over predicting.

Alok Ku Nanda, Soumya Dash, R. BhimaRao, Satya SaiSrikant [27] assessed the performance of the Pelton wheel turbine with different range of rotational speeds and varying loads using surface response methodology software Design Expert DX6 and their results achieved from the present investigation are discussed. The observed value for turbine shaft rotation in rpm indicated a very good fit for the response function equation. It is also found that the predicted value [29.46%] and the experimental value [29.52%] are very good fit for the efficiency of Pelton turbine.

Hence, in bringing technology of Pelton manufacturing to developing countries in a cost effective manner, it has been found that no significant work and particularly there was no institution or company that engaged in the development of small turbines in Ethiopia yet.

As a result, it has been found that it is more important to do the manufacturing, and experimental test of a Pelton hydro turbine and finally develop a manufacturing manual that will help in localization of the up to dated micro hydro Pelton turbine technology for hydro power project in Ethiopia.

Chapter Three

Manufacturing of Micro Pelton Turbine

An optimized Pelton turbine bucket design, with specifications of Power 2kW, Flow rate 20.8lit/sec, head 13.3m and PCD 212mm, which is used to model a 38.4kW which has two nozzles, was reduced to one nozzle to reduce manufacturing cost and its CAD model was used for 3D printing.

A methodology for manufacturing, as shown in Figure 3.1 were developed in order to manufacture the scaled down Pelton turbine.

Other turbine parts were designed and converted into manufacturing drawing as in appendix (A). The parts of the turbine in which manufacturing drawing is prepared for are Turbine Shaft with holder, Bearing Housing, Runner Plates, Shoulder, Spacers (Internal and External), Turbine Casing, Nozzle, Spear Valve, and Nozzle Controller.

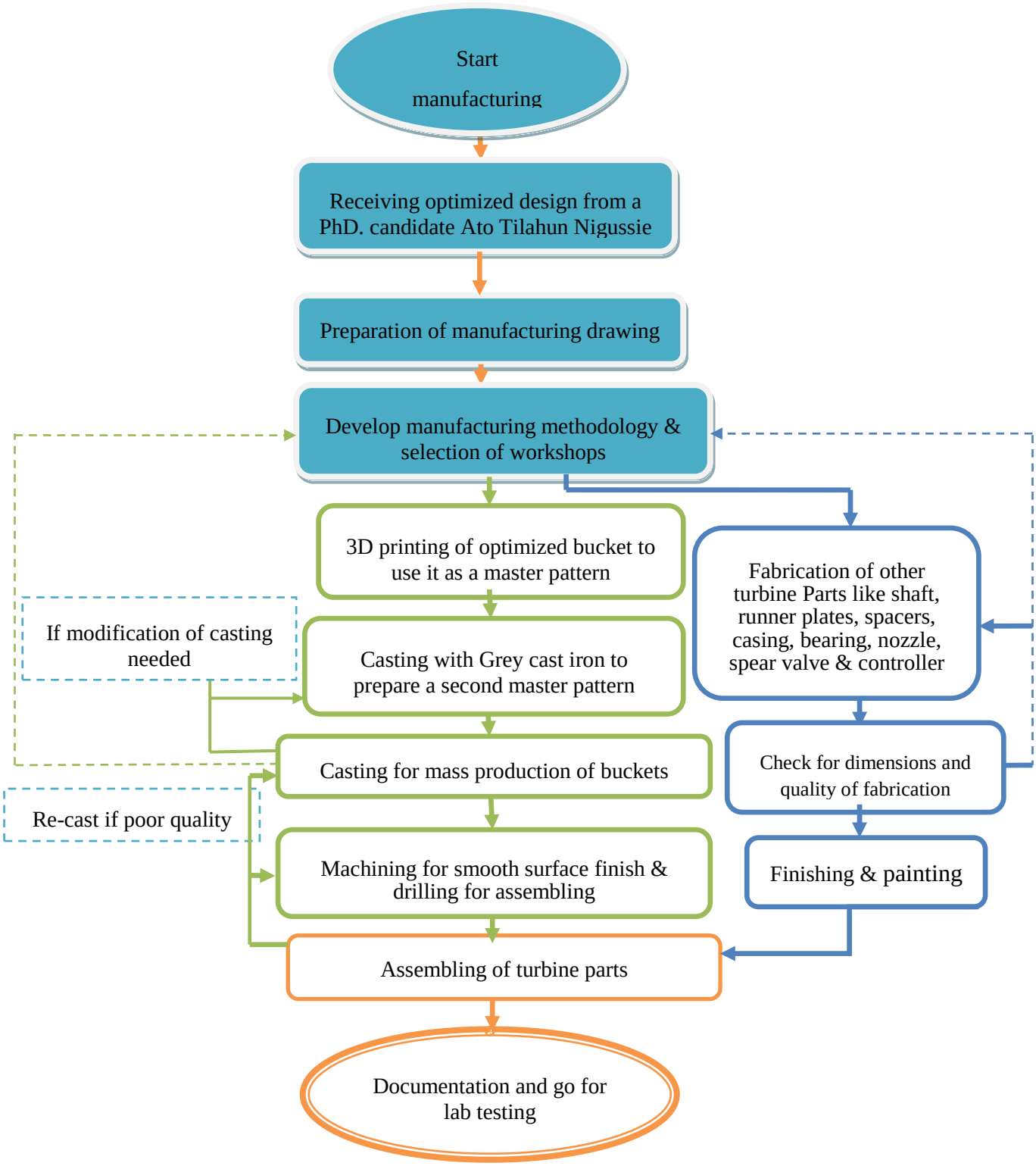

Figure 3.1: Methodology for manufacturing of Pelton Turbine

3.1 Material Selection

In selection of an appropriate material for construction of micro Pelton Turbine, the two main material properties required are corrosion resistance and load bearing capabilities. Although stainless steel is perhaps the most attractive option for this application, it is among the most difficult materials to work and manufacture with, making it very costly and time consuming to produce turbine parts from. Consequently, aluminium has been chosen to build the main body of the turbine, which is Turbine Bucket, due to its resistance to corrosion, cheap cost and suitable structural properties for turbines with 5KW maximum capacity [9]. More so, its forgiving nature and ease of manufacturing made it an ideal material to construct the buckets. Other Turbine Parts like shaft, spacers, casing, and nozzle assembly were fabricated from commercial steel mostly available in the local market.

In order to obtain a pattern dimension, for the metal being used (in this paper aluminium) as stated in table 3.1 multiplying the required bucket dimension by the shrinkage factor is necessary.

Table 3.1: Shrinkage factors for various metals [Jermey Take]

Metal	**Factor**
Aluminium	1.013
Brass	1.015
Bronze	1.017
Grey cast iron	1.009
Plain carbon and low allow steels	1.017
High alloy steels	1.023

3.2 Pelton Turbine Parts Manufacturing

In order to manufacture, manufacturing procedures for a micro Pelton turbine components described in Figure 3.1 were followed. Then as built in manufacturing drawings were developed to fabricate turbine components as attached in Appendix (A). SOLIDWORKS were used in the development of the drawings.

The fabrication of the buckets were made in a private company called Arefeayne Kasahun crafts and foundry works Plc. because of their in depth experience and facility in casting. The remaining components of the turbine were fabricated in a private company called TiGro Power Electromechanical and Alternative Energy Plc.

Assembling and performance testing of the turbine were made in AAiT hydraulics laboratory.

3.2.1 Pelton Turbine Bucket Manufacturing

CAD model of optimized bucket shown in Figure3.2 below was received from PhD Candidate, Ato Tilahun Nigussie. This 3D CAD model was used to print the Bucket to use it as a master pattern for casting of the buckets.

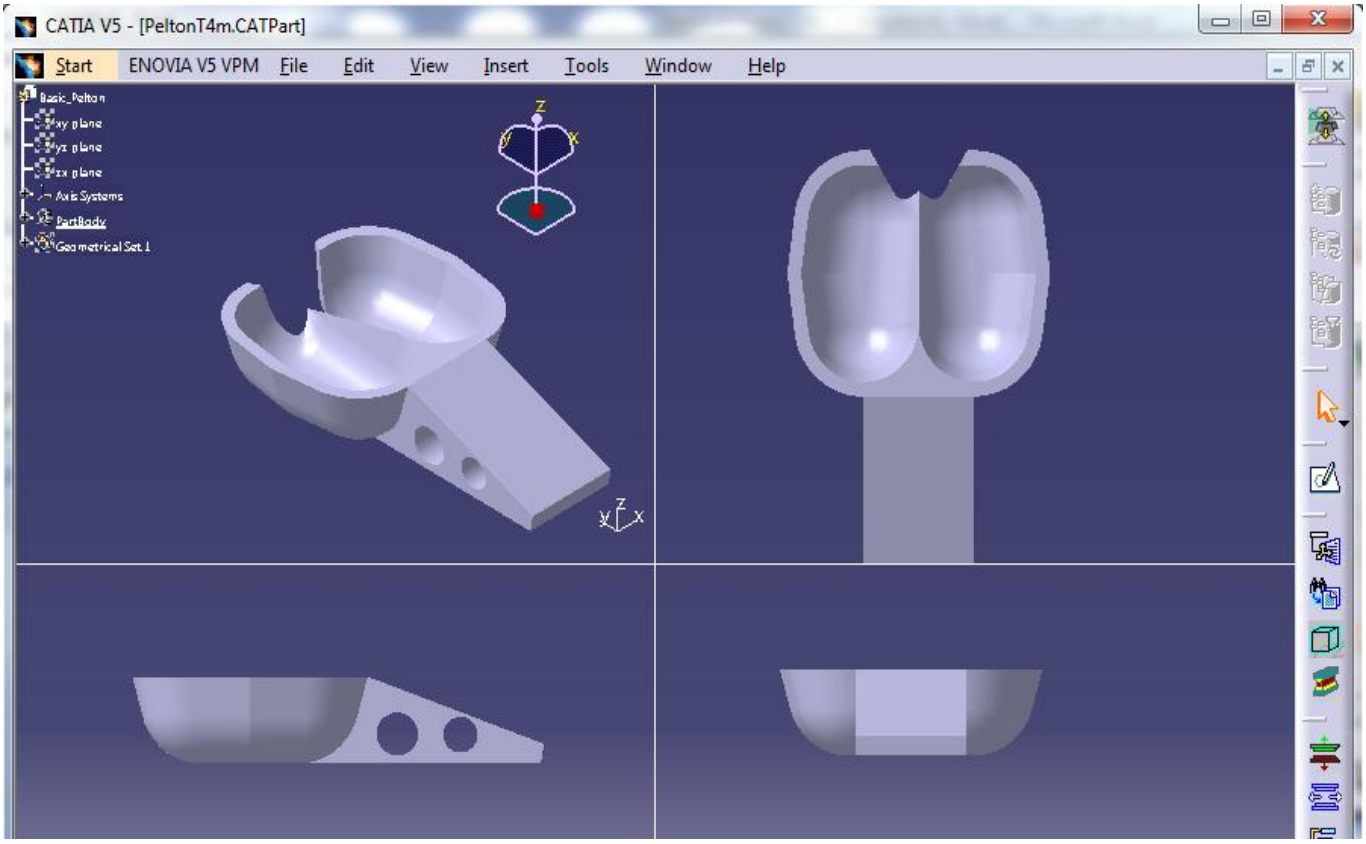

Figure 3.2: Optimized Pelton bucket designed by Tilahun Nigussie

To fabricate the turbine bucket, which is the most critical part of Pelton turbines, using a 3D printer to get a master pattern were crucial as the quality of making a wood, epoxy, aluminium or other materials is poor and may result in a reduction of hydraulic efficiency.

Thus it has been decided to use 3D printing technology to get an exact and best quality pattern for casting of buckets as far as it withstands the hitting load during sand mould preparation. Three institutions have been selected in Addis Ababa that has 3D printer, Fablab Addis, icogLabs and MoST. Fablab Addis's printer was not working due to a failure in its nozzle and it has been tried to use icogLabs printer.

The result of icog Labs bucket pattern was unfortunate as shown in Figure3.3 below. Because of the complex geometry of the bucket, their printer failed in its support printing part, which gives the lab a lesson to upgrade/import another high capacity 3D printer.

Figure 3.3: Photography of failed 3D printed optimized Pelton bucket in icogLab's 3D Printer

Finally, the prototype runner bucket was imprinted with an efficient 3D Printer from FDRE, Minister of Science and Technology, MoST as shown in Figure3.4. This model was then used as the master pattern to cast with grey cast iron and then using both the 3D printed plastic and the casted grey cast iron buckets as master patterns, the required quantity of bucket runners were casted by sand casting with Aluminium.

A) B) C)

Figure 3.4: Photography of 3D printed optimized Pelton bucket A) Isometric View B) Front View C) Back View

Material Properties of Raw Materials

To use the 3D printed out bucket as a master pattern for casting, it should bear up the repeated hammering load in the mould preparations in the sand formwork and should not be broken in leaving out from the sand mould. More so, it must leave exact shape cavity in the sand to pure

the molten aluminium. Hence its mechanical properties should be considered before deciding to select 3D printing technology than other pattern development techniques.

Therefore, considering mechanical property of the plastic material which was used in pattern development using 3D printing is a must. As per [5], the mechanical properties are to be tensile strength of 36MPa and flexural strength of 52MPa. For 7033-T6 Aluminium alloy, tensile strength is 518MPa and flexural strength is 41MPa [6]. Thus, the flexural strength, which is the essential property, of both materials is nearly similar with casting.

Hence, the thermoplastic ABS-P430 material as shown in Figure 3.5 can withstand the load and can even be used as a bucket material for Pico Pelton turbines. Although it could not be used as bucket material for this thesis research instead of aluminium as there were not sufficient raw material in MoST's stock and could not import it because of time limitation, it has indicated and given clues for future study area in studying its mechanical design and its hydro-economics for Pico/micro turbine applications.

Figure 3.5: Photography of material specification used in 3D Print of optimized Pelton bucket in MoST

The 3D Printed bucket runner was used as a pattern for sand casting of the buckets and finally it was used as a reference to check out the dimensions of the casted buckets.

Procedure of Casting

The procedure of casting to manufacture Pelton bucket were sand box preparation, pouring of molten aluminum, machining as described below;

Sand Box Preparation

A play wood form work is used to cast the lower part and upper part of the bucket using the 3D printed model and the casted grey cast iron as a master pattern. The procedure of sand casting of Pelton bucket in a box is as follows,

1. A plywood has been used to make a 600x400x200mm cube to make lower and upper box;
2. Sand has been poured up to 100mm height and after inserting pattern and fill, the sand was gently hammered the till the top surface of the pattern;
3. Waited till the sand dried and removed the pattern gently to make second bucket;
4. The above steps were repeated for the same box for the next bucket and
5. The above steps were repeated while the pattern is in its upside down position.

Pouring of the Molten Aluminum

The two half compacted sand molds were combined together with fixing screw in the form works, then a molten Aluminum is poured in to the sand mold to create the buckets.

After casting, machining work is done for smooth surface and to drill the holes to fix it to the runner plates since the molds are slightly irregular compared to the 3D printed plastic mold as shown in Figure 3.6.

Figure 3.6: Photography of casted buckets before machining

Machining of the Buckets

The external surface, internal surface and handle of the buckets were machined with grinding machine and then rotor grinding was used to surface the internal part of the bucket. Finally, file and sandpaper were used to make smooth and fine surfaces as shown in Figure 3.7.

Cutter machine was used in addition to the grinding, rotor and file machines and tools to make the part of the bucket.

Figure 3.7: Photography of casted Buckets after machining

Drilling of Buckets

Drilling of buckets to fix in the runner plates were made in two steps.

First the upper hole was drilled as per the plastic 3D printed model with milling machine as shown in Figure 3.8 secondly all buckets were fixed in the runner plates and then the lower holes of the buckets were drilled as per the previously drilled holes in the runner plates with drilling machine.

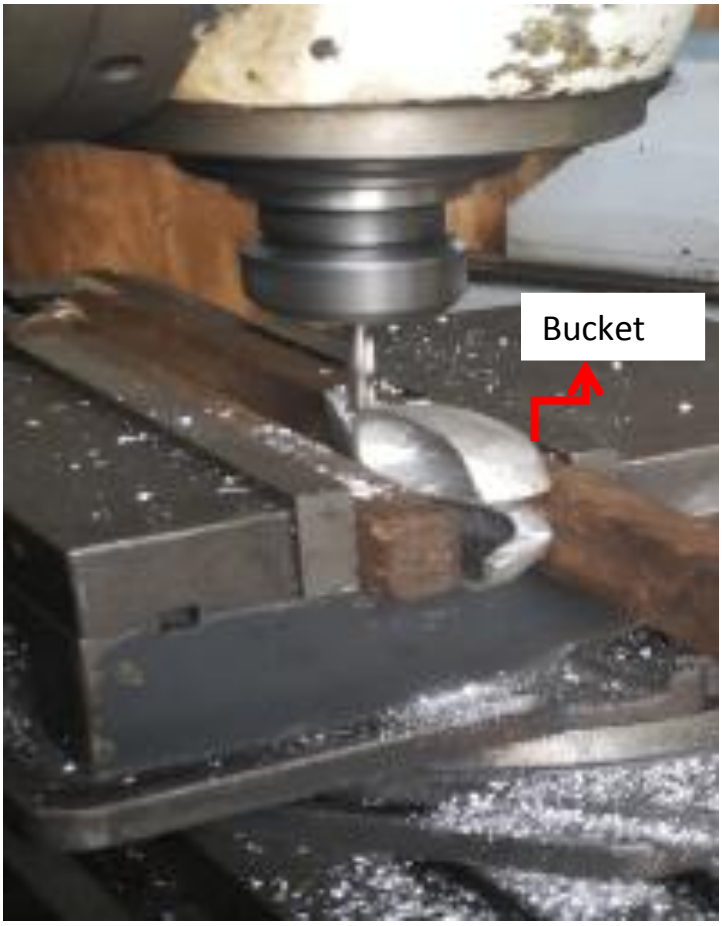

Figure 3.8: Photography of drilling of casted buckets

3.2.2 Manufacturing of Micro Pelton Turbine Casings

3.2.2.1 Sizing of Turbine Components

Sizing of other turbine parts depends on the pitch circle diameter (PCD) of the optimized bucket as shown in Figure3.9. After receiving Turbine optimized bucket with PCD of 212mm and other

parts design, a manufacturing drawing as seen in Appendix(A) were developed for the Optimized bucket considering casting tolerances for Aluminium casting which is 0.05% of PCD [28].

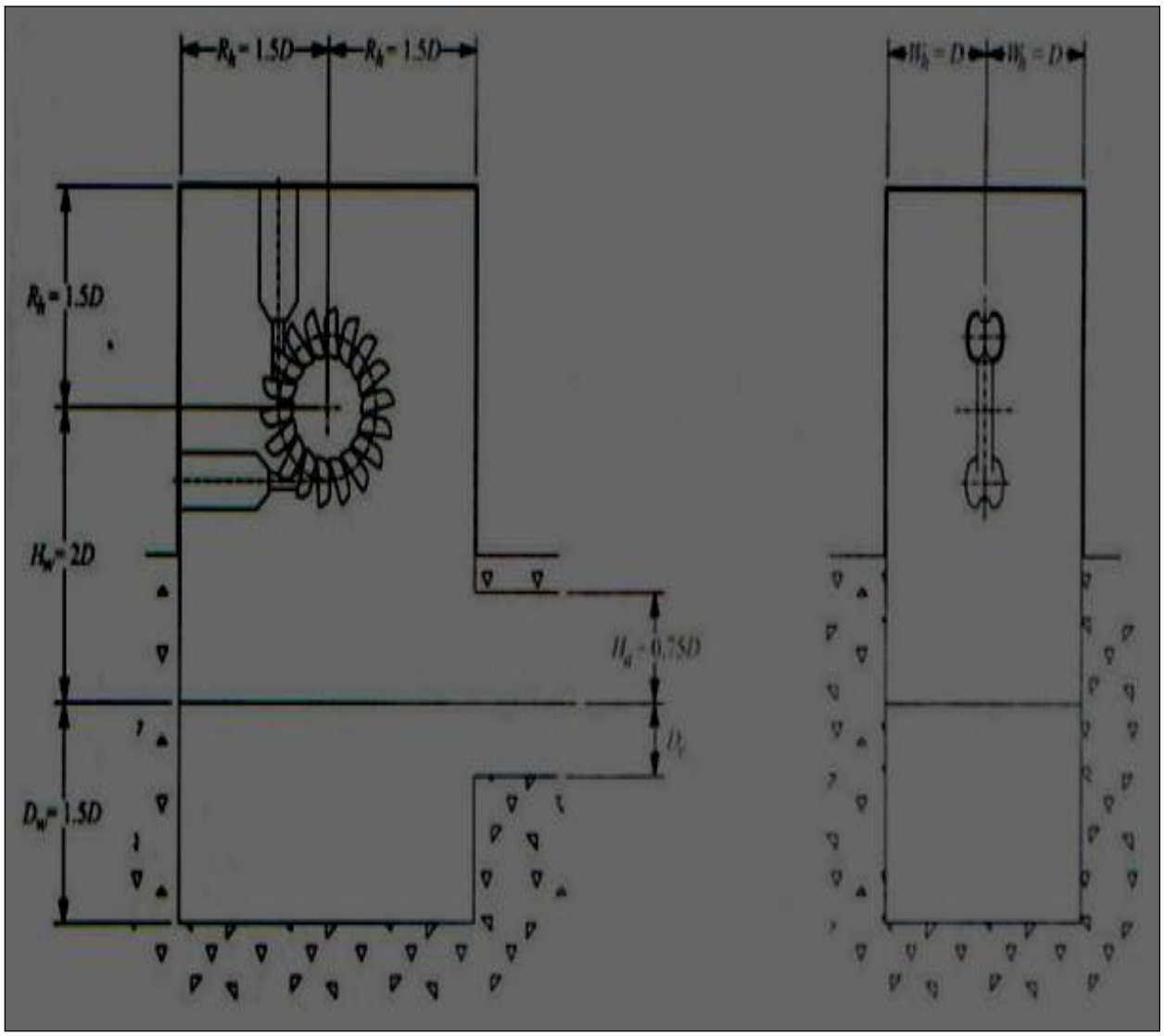

Figure 3.9: Dimensions of the Turbine Parts to fabricate casings [Jermey Thake].

The result dimensions of lower casing and upper casing of turbine parts are tabulated as shown in Table 3.1.

Table 3.2: Dimensions of the Turbine Parts [Jeremy Take]

Turbine Part	Parameters, Formula	Calculation	Dimension/Result by rounding to possible dimension for manufacturing	Unit
Upper Casing	Height of upper casing, h_u=1.5D	h_u=1.5*212	32	mm
	Width of upper casing w_u= 2D	w_u = 2*212	42	mm
	Length of upper casing l_u= 3D	l_u=3*212	64	mm
	Position of center of nozzle along the length, a=(1.5*D)-(0.5*D)=D	a=1*212	21	mm
	Position of center of nozzle along the width b=D	b=212	21	mm
Lower Casing	Height of lower casing, h_l=3.5D	h_l=3.5*212	74	Cm
	Width of lowercasing w_l= 2D	w_l = 2*212	42	Cm
	Length of lower casing l_l= 3D	l_l=3*212	64	Cm
	Position of center of nozzle along the height from top, c=0.5*D	c=0.5*212	106	Mm
	Position of center of nozzle along the width d=D	d=212	212	mm
	Position of center of Discharge from the bottom e=1.5*D	e=1.5*212	318	mm

3.2.2.2 Turbine Casings

The turbine's upper and lower casing are manufactured by cutting sheet metal to its shape and size with shearing machine, then parts has been bended at right angle with mechanical bending machine and drilling operation was made with drilling machine.

Lastly, arc-welding machines with electrodes make the welding of the sheet metal to fabricate the bottom and upper casing. The front part of upper casing was made with clear glass of 5mm thickness to visually see the operation of the turbine.

An angle iron of 50x50x5mm was used to support the bearing with housing to support the load of shaft assembly.

The thickness of the sheet metal used to fabricate the bottom casing is 6mm to support the shock and self-weight of the turbine but the upper part was made with a 2mm thick sheet metal to reduce the overall weight and cost of the turbine.

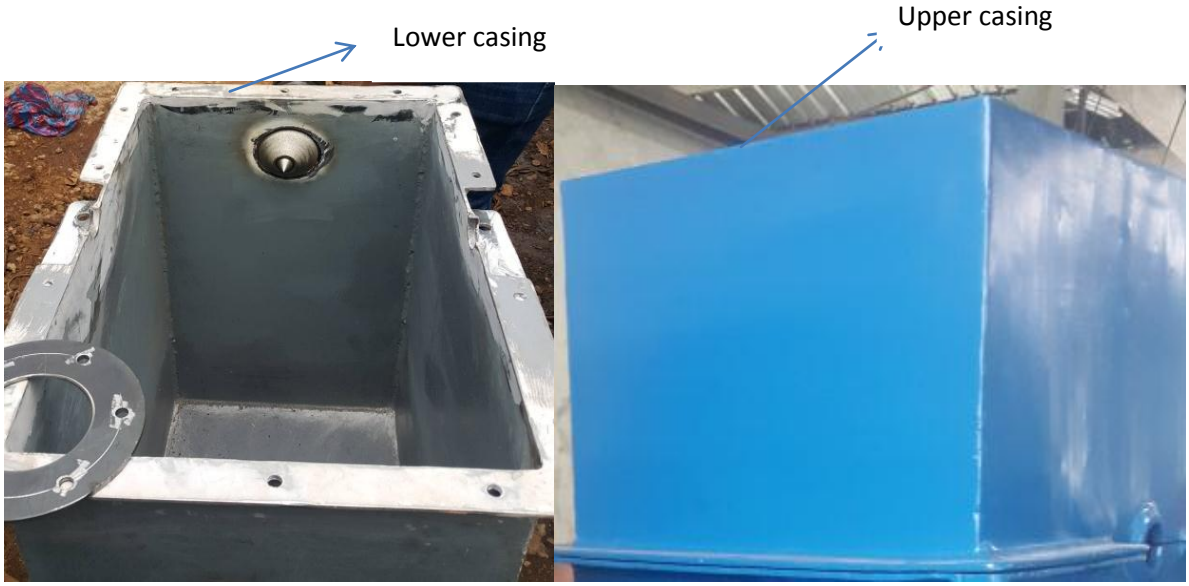

Figure 3.10: Photography of upper and lower casing of modeled turbine

Steps in Casing Fabrication

Shearing: a sheet metal of 6mm thick was sheared to the required lengths to make the bottom casing and 2mm thickness to make a casing using mechanical shearing machine.

Bending: the sheared sheet metals were bended at right angle and made ready for welding using mechanical bending machine.

Welding: using arc welding, the bended sheet metals were welded internally and externally to prevent water leakage and both bottom and top casings were made except one front surface of top cover that was covered by a glass instead of sheet metal.

Frame welding: Drilled flat bars were welded at the top end of the bottom casing and at bottom end of the top casing. An inner tube was used in the frames as gasket to prevent water leakages.

Nozzle Entry drilling and fixing: a hole of 100mm diameter was drilled with oxyacetylene at the bottom casing at 106mm from its top end. A 15mm thick, 120mm diameter flange with 6 holes of 12mm diameters was welded in the drilled hole. Another flange of 6mm thick was welded with the nozzle and then the nozzle was put in place at required clearance with bucket using the flanges with M12bolts.

Outlet drilling: in the opposite but lower than the nozzle entry, a hole was drilled at 212mm diameter using oxyacetylene that was used as an outlet for water.

Glass fixing: in order to visualize the operation of the Turbine, the front side of the top casing of the turbine was covered with a 5mm thick clear glass instead of sheet metal.

3.2.3 Manufacturing of Turbine Runner Plates

Turbine runner plates are the second sensitive part of the turbine components next to runner buckets as the two plates has to fix perfectly which influences the alignment of the buckets that result in loss of efficiency. The runner plates are used to transfer the rotational motion of the buckets to the shaft.

Thus, the plates were created using lathe machine, the central hole is bored using boring machine, and other holes are made using a vertical drill machine that has a divider tool to perfectly locate the holes locations.

Procedures of Runner Plate Fabrication

Cutting- the runner plates were made with 4mm thick sheet metal cut circularly with flame cutting, oxyacetylene.

Turning- the cut sheet metal with flame cutting could not be exact circular and the circular shape was maintained using lathe machine's turning operation and the central hole to fix to the shaft was made with same machine by the boring operation.

Punching of center hole- by first make a center line using marking tool and along this center line mark the first big hole at the exact position was punched and after that using the same center the first small hole was line marked and punched. These were used as starting positions of holes.

Punching of other holes using divider- using a divider tool which is attached in the drilling machine, other holes were marked and punched at 24^{o} in between each holes.

Drilling- by rechecking with the divider tool, drilling of each holes were made as shown in Figure 3.11.

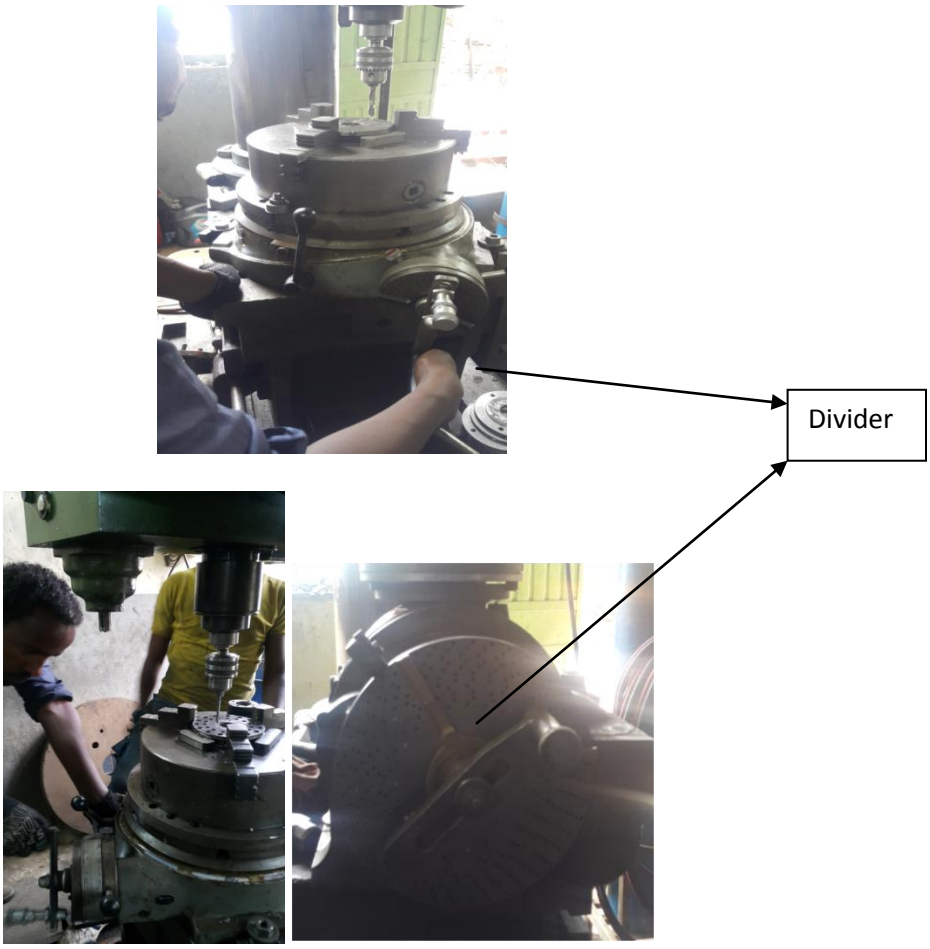

Figure 3.11: Photography of runner plates vertical drill machine with divider

3.2.4 External Holder and Spacers

Turbine external and internal spacer are used to hold and fix the runner plates in position and prevents the side way motion that may occur during operation of the turbine and hence, the spacers helps to transfer the rotational motion of the buckets and runner plates to the turbine shat efficiently.

Figure 3.12: Photography of external holder

Figure 3.13: Photography of spacers

Spacers were manufactured by using lathe machine's turning; facing and boring operations and its key ways are made with milling machine as shown in Figure 3.13.

3.2.5 Turbine Shaft and Bearings

Turbine shaft is used to transfer the rotational motion and torque created in buckets to a generator to generate power.

A 70mm diameter and 900mm long solid steel has been used to produce a turbine shaft and using lathe-turning operation a stepped shaft was created. Chamfering is made on the shaft on the same machine but key ways were created using milling machine.

Holder part of the shaft is used to hold all the spacers and runner plates and prevent the side way motion of all these parts of the turbine. It is fabricated by turning operation of the lathe machine which makes the shaft a stepped shaft.

Figure 3.14: Photography of Turbine Shaft

Slot making Procedures

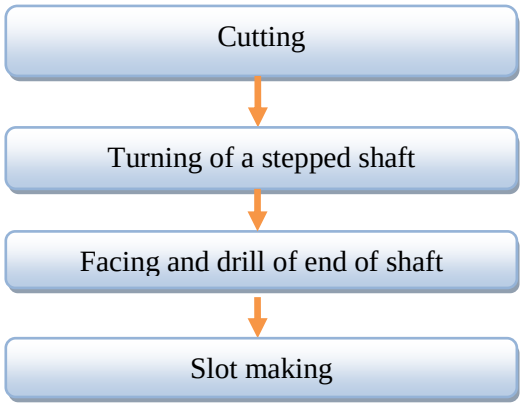

Figure 3.15: Procedures taken for slot making

Cutting: - a 1000mm length and 80mm diameter solid shaft is cut by a power hacksaw to a length of 800mm.

Turning: - the 80mm diameter solid steel shaft is turned to reduce the shaft diameter from one end to 30mm up to a length of 100mm and again turning was done from the other end to a length to make the shaft diameter 30mm. the remained 80mm diameter was reduced to 75mm to make a stepped shaft that is used as a shaft holder and all turbine parts were fixed in this holder with four M6 bolts in its slots. This holder is used to prevent the longitudinal movement of the turbine parts and thus it is used to transfer the rotational motion of the buckets to the shaft efficiently.

Slot making: - drilling in the stepped shaft part i.e. on the holder was very difficult and was replaced by slot as shown in figure below. The slot is used to fix the M6 bolts to hold parts of the turbine like external spacer, internal spacer, and runner plates.

Figure 3.16: Photography of Turbine Shaft Slot

3.2.6 Nozzle, Spear Valve and its Adjustment

Outer facing: a solid shaft of 105mm diameter and a length of 215mm were cut with a power hacksaw and its external surface was faced using a lathe machine until its diameter reached 100mm.

Cone shape facing: the tip of the nozzle was faced with a lathe machine to make a conical surface to make the included angle 90^{o}.

Boring: the first step in boring of the nozzle was to drill with a 30mm diameter drill bit and boring operation of lathe machine has been used to make an internal diameter of the nozzle 92mm and a length of 154mm.

Inner cone facing: the remaining 56mm length of the nozzle was bored at an angle to make a nearly conical surface and an included angle of $53^{o}$was made.

Spear Valve: a 45mm diameter solid shaft was used to make the spear vale. The first operation was to face the shaft a length of 180mm till the diameter becomes 24mm. The second operation was to make the head and tip of the spear valve by facing at different angles to make its head and 26.5^{o} angle was used to make its tip.

Bushing for axial movement of spear valve: a length of 30mm and diameter 35mm was used to make the bushing to support the axial motion of spear valve to keep its center. The shaft was

drilled at 25mm diameter drill bit in two parallel surfaces and screw was made in the drilled holes. Using these screwed holes, the bushing is suspended to the nozzle body using bolts. The bolts ware lastly welded to the nozzle body.

Bolt and nut for adjustment: a long bolt was welded to the end of the spear valve and this was inserted in a screw made bushing that was welded to a drilled elbow.

Handle: for ease operation of the spear valve and handle was prepared using plate and double nuts. The double nuts were first tightened in the long bolt which was welded to the spear vale and the plate drilled at its center and screwed was fixed to the long bolt. Finally two nuts were tightened after the plate.

A) Nozzle and Spear Valve front view b) Side View

C) Spear Valve and Nozzle assembled front View

Figure 3.17: Photography of a) Nozzle b) Spear Valve and c) Assembled Spear Valve and Nozzle

3.3 Assembling of the Turbine

The first step in assembling of the Turbine is to assemble the bucket holders as per listed items below using 4 M6 Bolts and nuts as shown in the figure below. The steps in order to assemble the modeled turbine are numbered below.

1. Preparation of shaft: lay down the shaft on leveled ground and fix the key on the key ways on the shaft at behind the external holder and on the center of the shaft where the runner plates, internal spacer, and external spacer are to be fixed.

2. Fixing of external holder to the stepped shaft: is used to hold the bucket assembly in place and then to prevent axial motion of the components. Insert the key in the shaft's key way and then insert the external holder. In the external holder insert 6long bolts to make ready for insertion of other components.

3. Fixing of runner plate: are used to hold the buckets in place. Insert one of the runner plates in the 6 long bolts till the plate latches to the external holder.

4. Fixing of internal spacer: is used to keep the space clearance of the runner plates. After inserting the one of the runner plate insert a key in the key way in the shaft and then insert the internal spacer.

5. Fixing of outer runner plate: after fixing of the internal spacer, insert the second runner plate.

6. Fixing of Buckets: buckets are used to exploit kinetic energy of water and hence fixing of these buckets in the right place determines its efficiency. Using angle divider, fix the buckets with two bolts for each bucket.

7. Fixing of external spacer: fix the external spacer after fixing the second runner plate and tighten the nut to the design torque to fix all the components.

8. Tightening of M6 Bolts and nuts. Tightening all the bolts and nuts to the required torque is very crucial to prevent loosing and missing of water jet and there by breakage of components due to vibration in starting and at maximum torque.

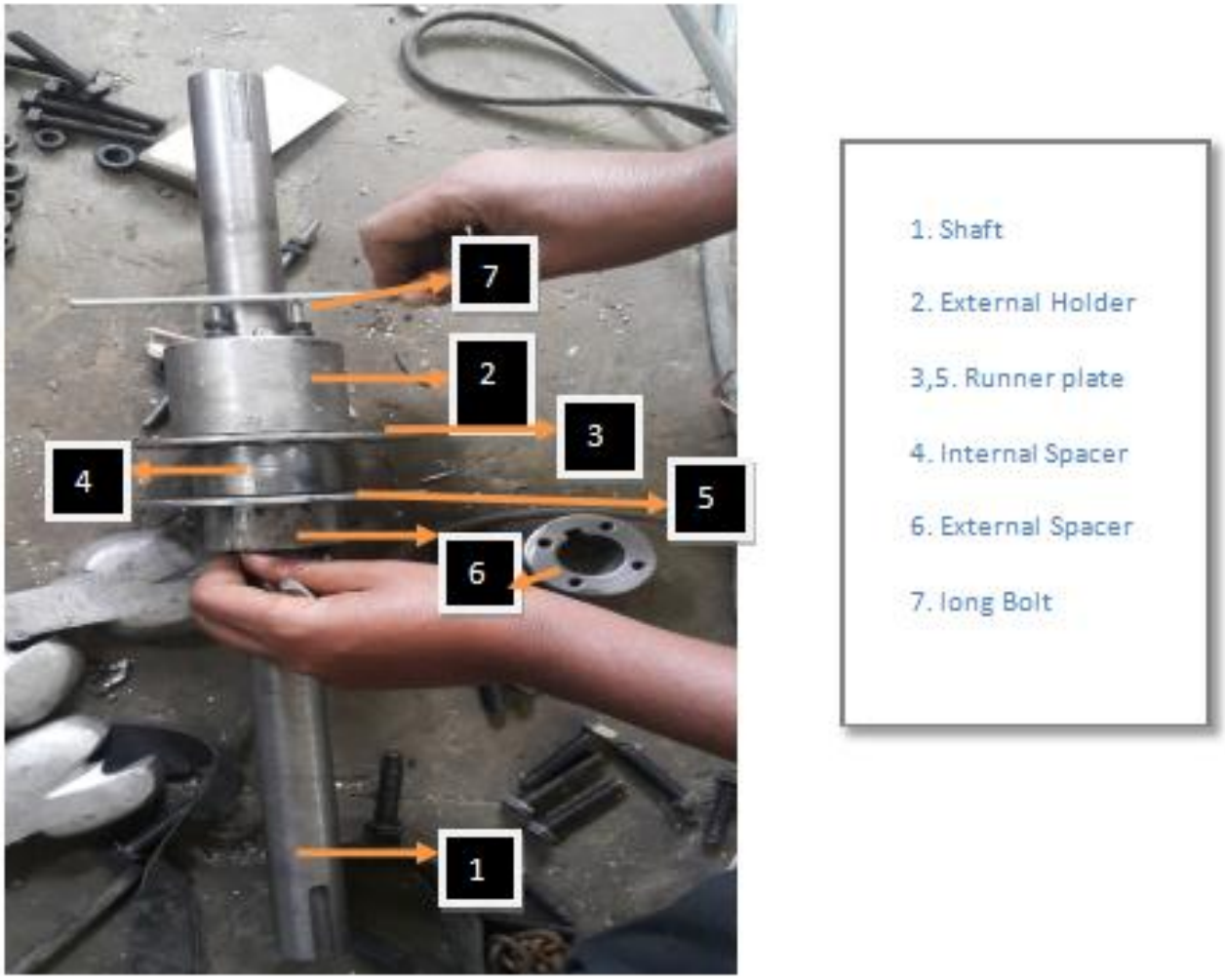

Figure 3.18: Photography of Assembled Turbine runner parts

The second step of assembling of Turbine is Fixing of Buckets in between the runner plates as shown in Figure 3.18.

*S*tep 1: Fixing of the buckets with M10 Bolts and nuts

The first step was fixing all of the buckets with M10 bolts, then angle between each buckets were made 24^{o} as shown in figure and then tightening of the bolts with the required torque was made lastly.

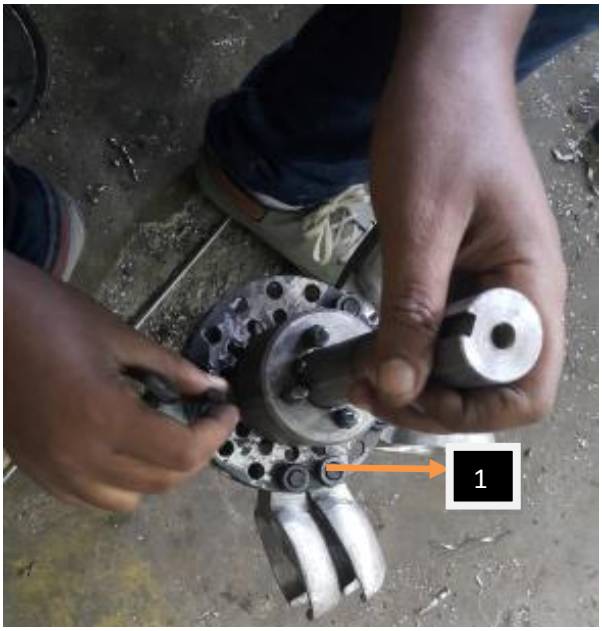

Figure 3.19: Photography of fixing of runner plates with M10 Bolts

Step2: Fixing of the buckets with M8 Bolts and nuts and then tightening of the bolts with the required torque was made lastly. In this step the distance between each bucket were set correctly.

Figure 3.20: Photography of fixing of bucket with M8 Bolt to set the distance between each bucket

Step3: Fixing of the bearings on assembled bucket. The turbine bearing was fixed in the shaft using hydraulic press machine as shown in Figure 3.21 with keys.

Figure 3.21:Photography of fixing of Bearing

Step4: Fixing of turbine assembled parts to the lower casing. After assembling the turbine components, the next step was to fix the assembled parts to the lower casing of the turbine and check for static and dynamic balance for stability.

Figure 3.22: Photography of Fixing of bucket and shaft assembly to lower casing

Step5: Assembling of Nozzle assembly on lower casing, the spear valve, nozzle, elbow, flow control adjuster, spear valve holder was assembled and fixed to the lower casing in the correct direction, alignment and at the Wright position from bucket as shown in Figure 3.23.

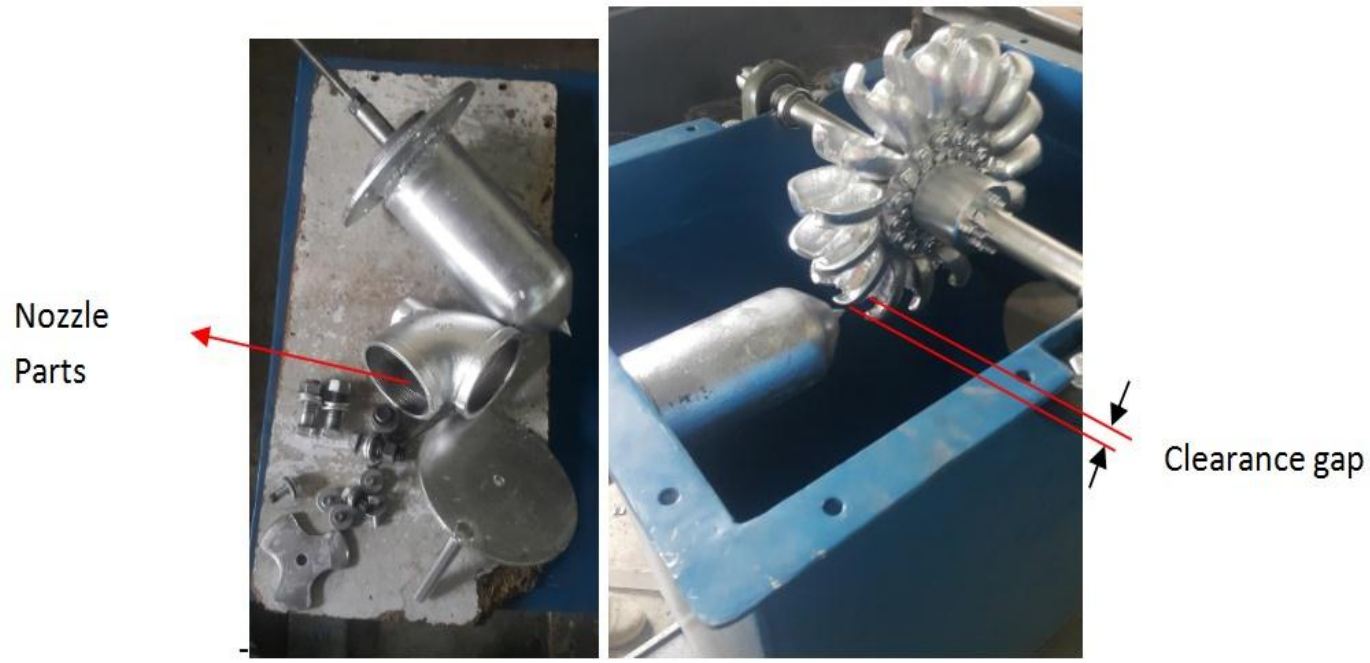

a) b)

Figure 3.23: Photography of fixing of nozzle assembly a) Nozzle Parts b) Nozzle, Assembled Bucket, Lower casing

Step6: Fixing of Upper Casing, finally the upper casing was fixed with lower casing using gasket to prevent leakage at the Wright torque as shown in Figure 3.24a and the final Pelton turbine product is shown in Figure 3.24b below.

Figure 3.24a: Photography of fixing of upper casing Figure 3.24b: Final product

After assembling the manufactured Pelton turbine, it is installed at AAiT hydraulics laboratory for performance testing of the turbine as shown in figure 3.25.

Figure 3.25: Fixing of the Turbine to test bench

3.4 Runner Assembly Balancing

All running machine parts should be balanced before use and hence pelton turbine buckets as a running machine part, its static balancing were done. Static balancing is insuring that the center of gravity of the runner lies on the axis of the shaft.

Static balancing were done by first fixing the runner assembly on lower casing and running the runner assembly slowly using electric motor with gearbox. The gearbox is used to reduce the speed of electric motor as dynamic balancing which needs high speed do not need to carryout for small size turbines [29].

The procedure used were first start the motor to run the runner assembly for a minute and start the motor and wait till the runner stops running and mark the bucket that directs downward. Repeat the above step several times and mark the buckets that directs downward for each running and observe that if the buckets that directs downward are different for every trials, it can be concluded that the runner is statically balanced. But in this research work, in four bucket direction, it was not balanced and welding of using Aluminum electrodes in the opposite direction of the respected unbalanced buckets. After repeating the same procedure for the third time, the manufactured runner were statically balanced with little vibrations remained that could not disturb the testing. It could not refine the vibration fully as we could not have the right balancing machine like car wheel balancing machine.

Chapter Four

Experimental Testing

In this chapter a laboratory experiment was done to evaluate the manufactured turbine by producing curves that shows its performance

Owing to the difficulties in the calculation of unsteady flow processes, previous studies of Pelton turbines are almost exclusively confined to experimental methods and model tests. The experimental investigations have been primarily related to the measurements of the jet and the water flow both in fixed and rotating buckets, while the model tests are mainly conducted for flow visualization and measurement of the system efficiency.

Experimental measurements of flows in Pelton buckets are associated with great hindrance because of the difficult access to the flow there. Therefore, only flow visualization on the interaction between the jet and the rotating buckets as well as on the exit flow out of the buckets could be accomplished in earlier investigations [25].

Experimental testing has been done in AAiT; Hydraulics Laboratory using COMESA is testing procedures [15]. Turbine characteristic curves were drawn using Excel spreadsheet using the measured and calculated variables of the turbine.

A methodology for testing, as shown in Figure 4.1 were developed to test the turbine which is a scaled down designed model.

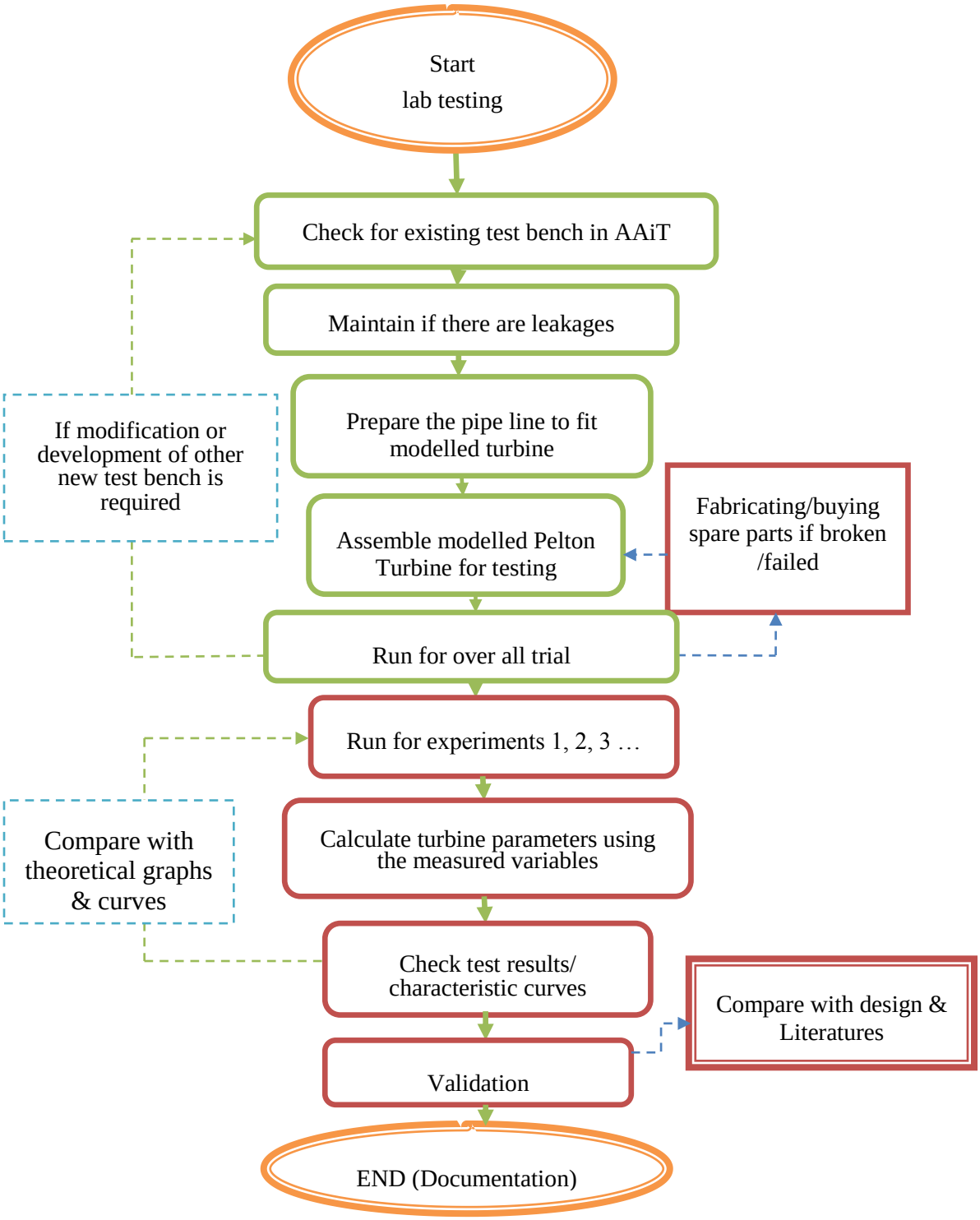

Figure 4.1: Methodology for Lab Testing

4.1 Test Setup

There are two pumps in AAiT hydraulics Lab. The first pump delivers to the lower tank, which is 4mt high, creating a 4mt static head and the second pump delivers to the upper tank, which is 15.4Mt high. The second pump, which was planned to carry the turbine test was failed and could not be maintained. Thus, we were forced to buy a pump to deliver water from the lower tank to the upper tank to create the designed head.

The schematic diagram of test setup used for this paper is shown in Figure 4.2.

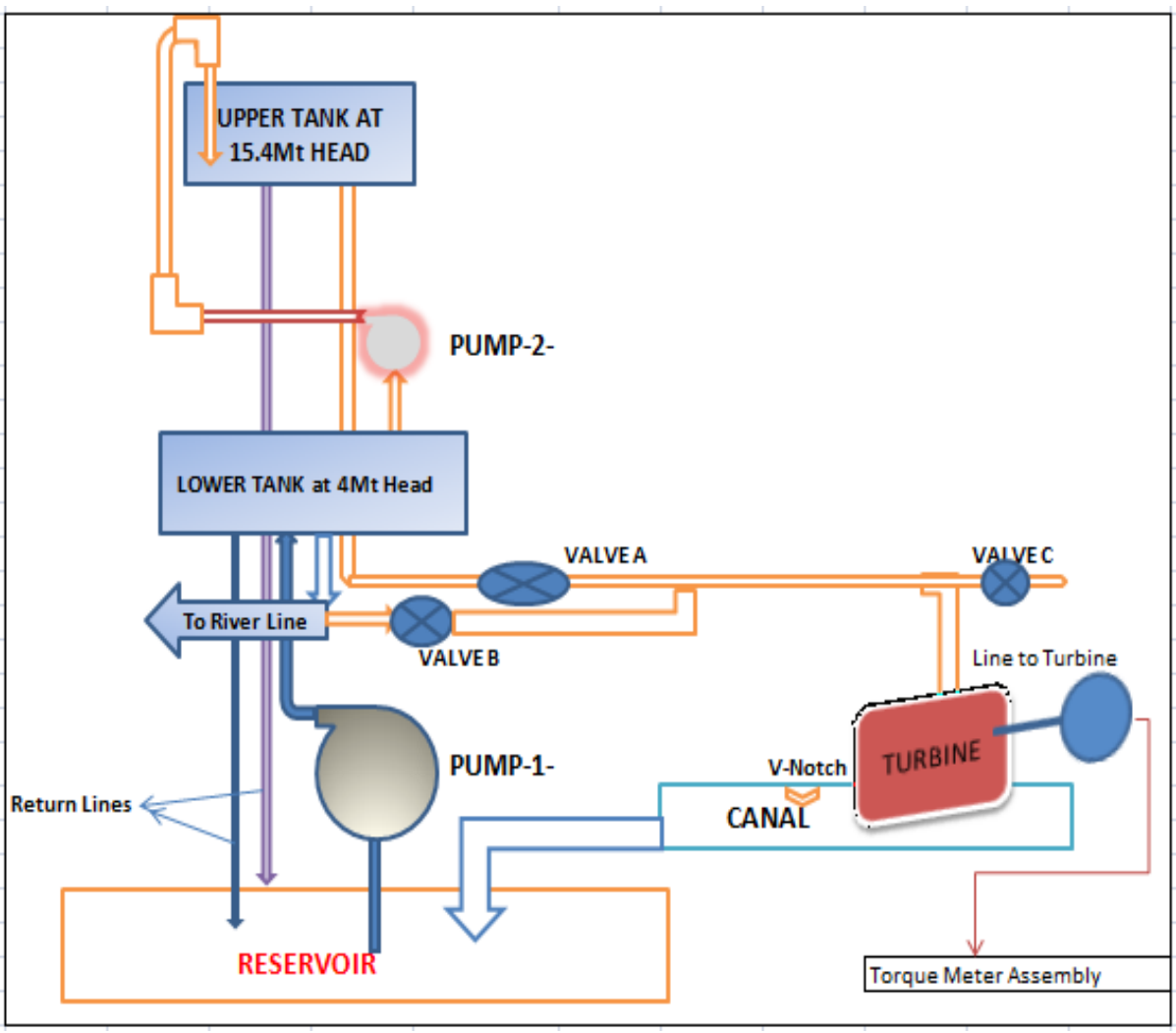

Figure 4.2: Schematic diagram test setup used in AAiT Hydraulics Lab

4.2 Instrumentation and Calibration

In order to complete this demonstration number of equipment were used. The equipments used in this performance test were

1. Manufactured Pelton Turbine;
2. Pressure gage to measure the pressure to calculate the static head;
3. V-notch height measurement to measure and calculate the volume flow rate;
4. Tachometer to measure the rotor speed;
5. A stopwatch to determine the flow rate of water which is also used to calibrate the V-notch as its calibration and
6. Torque meter to measure the torque output of the turbine.

The pressure gage, stopwatch, and tachometer used during this test were new and were calibrated as per their manuals. Calibration of V-notch height was done using the stopwatch, digital weight meter, and tank. The tank empty weight were measured using the digital weight meter and the timed collected water were weight and the balance weight were compared with the V-notch height measured and the v-notch were calibrated as per the procedures as attached in annex.

4.3 Experiment Types

Two experiment types were carried out to generate the characteristic curve of manufactured Pelton turbine in order to evaluate its performance:

4.3.1 Experiment 1: No load test of Pelton turbine

The objective here is to determine the correct alignment of nozzle with bucket, gap between each bucket, to check its dynamic balance, to check bearing alignment and rigidity by measuring and comparing the turbine's RPM with calculated values.

4.3.2 Experiment 2: Load Test of Pelton Turbine

4.3.2.1 Main Characteristics of Pelton turbine

The objective here is to determine the operating characteristics (Power, Torque, and Efficiency) of the manufactured turbine and compare it with the theoretical and simulation results.

A brake dynamometer was used in order:

1) To vary the speed of the turbine rotor from maximum speed (zero, torque) to minimum speed (rotor stalled / maximum torque) in stages

2) To measure the torque produced by the turbine rotor at each stage

A spear valve was used to change the volume flow rate through the turbine, allowing the above tests to be repeated at different flow rates. The handle plate in the spear valve controller has a mark rod to count the number of revolutions the handle rotates to divide the spear valve stroke length in equal 4 divisions.

From the readings obtained, graphs of Torque, Brake power and Overall Efficiency against rotor speed were plotted to show the operating characteristics of the Pelton Turbine using Excel.

The basic parameters that define the turbine performance are

1) Volume flow rate (Q)

2) Inlet Head (H_i)

3) Hydraulic Power (P_h)

4) Torque (T)

5) Brake Power (Output Power) (P_b)

6) Overall Turbine Efficiency (η_o)

Test Procedure

1. Check the reading of the pressure gage, it should read zero initially
2. Slowly open the spear valve, rotate the handle 7 revolutions, and set the spear valve at 25% open position.
3. Record the speed and tighten the spring in the brake drum and record the weight reading in the weight balance.
4. Rotate the handle next 7 revolutions, and set the spear valve at 50% open position.
5. Record the speed and tighten the spring in the brake drum and record the weight reading in the weight balance.
6. Rotate the handle next 7 revolutions, and set the spear valve at 75% open position.
7. Record the speed and tighten the spring in the brake drum and record the weight reading in the weight balance.
8. Rotate the handle next 7 revolutions, and set the spear valve at 100% open position.
9. Record the speed and tighten the spring in the brake drum and record the weight reading in the weight balance.
10. Repeat step 2 to step 9 for 3 trials to take the average.

4.3.2.2 Useful Equations

Each of these parameters is considered in term:-

The flow rate of fluid through the turbine is the volume passing through the machine per unit time.

$$Q = \frac{V}{t}\left[\frac{M^3}{S}\right] \quad \text{----------4.1}$$

The term 'Head' refers to the elevation of a free surface of water above or below a reference datum. In the case of a Pelton Turbine, we are interested in the head of the water entering the spear valve, which of course has a direct effect on the characteristics of the unit. In this turbine the head of water is generated by the static head of the upper tank. A new water pump was bought and was used to raise the water from the lower tank to the upper tank to get the required head as the second pump of the existing was failed.

The Bourdon pressure gauge measures the inlet pressure, p_i, in relation to atmospheric pressure. As the runner and the outlet of the turbine are at atmospheric pressure, it can be assumed that the reading given by the gauge is the pressure difference across the turbine. For the purpose of calculating the performance of the turbine the measured.

Pressure is converted to an equivalent head of water, H_i, as follows:

$$H_i = \frac{P_i}{\rho g} \quad \text{4.2}$$

Where: P_i −inlet pressure

ρ − Density

g −gravity of earth

The hydraulic power supplied by the water, P_h, can be calculated as

$$P_h = \rho g H_i Q \quad \text{4.3}$$

The mechanical power, P_b, produced by the turbine in creating a torque T on the brake at rotor speed N is given by

$$P_b = \frac{2\pi NT}{60} \quad \text{4.4}$$

The torque itself is given by the equation:

$$T = F_b r \quad \text{4.5}$$

Where r is the radius of the brake pulley and F_b is the Brake force

Where $F_b = (W_{s2} - W_{s1})$ and W_{s2} and W_{s1} are the readings on the two spring balances.

The Overall Efficiency of the turbine is determined from several separate efficiencies as follows:

Fluid friction 'losses' in the turbine itself, require a hydraulic efficiency η_h that is defined as:

$$\eta_h = \frac{Power\ Absorbed\ by\ the\ Rotor}{Fluid\ Power\ Supplied} \times 100\% \quad \text{4.6}$$

Mechanical losses in the bearings etc. require a mechanical efficiency η_m that is defined as

$$\eta_m = \frac{Power\ Supplied\ by\ the\ Rotor}{Power\ Absorbed\ by\ the\ Rotor} \times 100\% \quad ----------4.7$$

The dynamometer in the AAiT laboratory does not include direct measurement of mechanical power output Pm, but instead measures break force that is applied to the rotor via the band brake. A further efficiency is therefore required, expressing the friction losses in the brake assembly η_b that is defined as:

$$\eta_b = \frac{Power\ Absorbed\ by\ the\ Brake}{Power\ Supplied\ by\ the\ Rotor} \times 100\% \quad ----------4.8$$

The Overall Efficiency of the Pelton Turbine is the product of these individual efficiencies therefore is:

$$\eta_o = \eta_h \eta_m \eta_b \quad ----------4.9$$

$$\eta_o = \frac{Power\ Absorbed\ by\ the\ Brake}{Fluid\ Power\ Supplied} \times 100\% \quad ---------- \quad 4.10$$

$$\eta_o = \frac{2\pi \mathrm{NT}}{\rho g H Q} \times 100\% \quad ----------4.11$$

4.3.2.3 Turbine Operating Characteristic at constant speed

The objective is to investigate the performance of the turbine at constant speed. The turbines are generally designed to work at particular values of H, Q, P, N and η_o which are known as the designed conditions. But often the turbines are required to work at conditions differs from those for which they have been designed.

Therefore, it is essential to determine the exact behavior of the turbines under the varying conditions by carrying out tests. The results of these tests are graphically represented and the resulting curves are known as characteristic curves. One of these curves is the constant speed curves.

In order to draw these curves following procedure is adopted:

1. The constant speed was attained by regulating the gate opening thereby varying the discharge flowing through the turbine as the load varies. The head may or may not remain constant
2. The power developed corresponding to each setting of the gate opening was measured and the corresponding values of η_o are computed.
3. The total load capacity of the turbine, the percentage of full load may be computed from the measured power.

Observation

1. For each percentage of loads read the following parameters: Q, p, N, T and developed power P.
2. From the above reading parameters, the following parameters can be calculated: unit flow rate Q_u, unit speed N_u, unit power P_u and overall efficiency.

Test Procedure

1. Check the reading of the pressure gage, it should read zero initially
2. Slowly open the spear valve until the turbine speed 300RPM.
3. To vary the load tighten the spring in the brake drum and adjust the flow rate to keep the speed constant at 300RPM.
4. Record the weight reading and the flow rate/ spear valve open position.
5. Repeat steps 2 to 4 for different speeds 500, 650, 950, and 1100RPMs and record the weight reading and the flow rate/ spear valve open position.
6. Repeat step 2 to step 5 for 3 trials to take the average.

4.4 Result Data

In this section, measured and calculated variables of the manufactured turbine were presented. Characteristic and performance curves of the turbine were generated from these variables in the next chapter.

Table 4.1: Measured and calculated parameters at 100% Spear Valve Open Position

Parameters		Trial								
		1	2	3	4	5	6	7	8	9
Sppe, N	rpm	0	300	500	650	950	1100	1200	1250	1430
Pressure, P	N/m^2	131	131	131	131	131	131	131	131	131
Volume Flow Rate, Q litres/sec (measured using Calibration of v-notch)	L/s	10.41	10.41	10.41	10.41	10.41	10.41	10.41	10.41	10.41
Angular Speed, ω	rad/sec	0.00	31.42	52.37	68.08	99.50	115.21	125.68	130.92	
Net spring balance, reading (Ws1-Ws2)	N	122.28	89.47	74.87	66.33	30.33	16.33	8.00	0.00	
Torque $Te=R_w*(Ws_1-Ws_2)$, $R_w=0.150Mt$	N.m	18.34	13.42	11.23	9.95	4.55	2.45	1.20	0.00	
Inlet Head, H (meters)=P/rg	m	13.34	13.34	13.34	13.34	13.34	13.34	13.34	13.34	
Experimental Power, Pe = Tω	Watt	0.00	421.66	588.08	677.36	452.71	282.26	150.82	0.00	
Theoretical Power, Pt=(mw) Co^2 k(1-k)(1-cosβ2)	Watt	0.00	741.60	1016.98	1108.53	995.94	791.80	600.95	489.10	0.00
Theoretical Torque, Tt = (mw) Rw Co(1- k)(1-cos β2)	N.m	29.87	23.60	19.42	16.28	10.01	6.87	4.78	3.74	0.00
Input Power, Pin = ρ*g*Q*H	Watt	1362.31	1362.31	1362.31	1362.31	1362.31	1362.31	1362.31	1362.31	
Experimental Overall efficiency, ηo =Pe/Pin		0.00	0.31	0.43	0.50	0.33	0.21	0.11	0.00	
Bucket Speed, m/s	Co= ωr	0.00	3.33	5.55	7.22	10.55	12.21	13.32	13.88	
Speed ratio, k	k =U/C0	0.00	0.21	0.35	0.45	0.66	0.77	0.84	0.87	
Theoretical Hydraulic efficiency, η_{hy} =2*k*(1-k)*(1-cosβ)		0.00	0.57	0.78	0.85	0.76	0.60	0.46	0.37	0.00
Theoretical Overall efficiency, η_{tO} =η_{hy}*0.60		0.00	0.34	0.47	0.51	0.46	0.36	0.28	0.22	0.00

Table 4.2: Measured and calculated parameters at 75% Spear Valve Open Position

Parameters		Trial								
		1	2	3	4	5	6	7	8	9
Sppe, N	rpm	0	320	500	650	960	1020	1100	1200	1430
Pressure, P	N/m^2	135	135	135	135	135	135	135	135	135
Volume Flow Rate, Q litres/sec (measured using Calibration of v-notch)	L/s	7.80	7.80	7.80	7.80	7.80	7.80	7.80	7.80	7.80
Angular Speed, ω	rad/sec	0.00	33.51	52.37	68.08	100.54	106.83	115.21	125.68	149.77
Net spring balance, reading (Ws1-Ws2)	N	110.33	66.27	60.13	55.73	18.67	15.33	0.00		
Torque Te=R_w*(Ws_1-Ws_2), R_w=0.150Mt	N.m	16.55	9.94	9.02	8.36	2.80	2.30	0.00		
Inlet Head, H (meters)=P/rg	m	13.75	13.75	13.75	13.75	13.75	13.75	13.75	13.75	13.75
Experimental Power, Pe = Tω	Watt	0	333.1288	472.3473	569.1209	281.5232	245.7044	0		
Theoretical Power, Pt=(mw)Co^2 k(1-k)(1-cosβ2)	Watt	0	580.8029	759.8054	827.7398	734.1165	679.5635	588.4457	445.0088	0
Theoretical Torque, Tt = (mw)Rw Co(1- k)(1-cos β2)	N.m	22.36	17.32981	14.50933	12.15894	7.301445	6.361286	5.10774	3.540808	0
Input Power, Pin = ρ*g*Q*H	Watt	1052.12	1052.12	1052.12	1052.12	1052.12	1052.12	1052.12	1052.12	1052.12
Experimental Overall efficiency, ηo =Pe/Pin		0.00	0.32	0.45	0.54	0.27	0.23	0.00		
Bucket Speed, m/s	Co= ωr	0	3.55	5.55	7.22	10.66	11.32	12.21	13.32	15.88
Speed ratio, k	k =U/C0	0	0.22	0.35	0.45	0.67	0.71	0.77	0.84	1.00
Theoretical Hydraulic efficiency, η_{hy} =2*k*(1-k)*(1-cosβ)		0	0.59	0.78	0.85	0.75	0.70	0.60	0.46	0.00
Theoretical Overall efficiency, η_{tO} =η_{hy}*0.60		0.00	0.39	0.50	0.55	0.49	0.45	0.39	0.30	0.00

Table 4.3: Measured and calculated parameters at 50% Spear Valve Open Position

Parameters		Trial								
		1	2	3	4	5	6	7	8	9
Sppe, N	rpm	0	306	490	653	943	980	1000	1040	1400
Pressure, P	N/m^2	140	140	140	140	140	140	140	140	140
Volume Flow Rate, Q litres/sec (measured using Calibration of v-notch)	L/s	5.20	5.20	5.20	5.20	5.20	5.20	5.20	5.20	5.20
Angular Speed, ω	rad/sec	0.00	32.05	51.32	68.39	98.76	102.64	104.73	108.92	146.63
Net spring balance, reading (Ws1-Ws2)	N	59.00	37.07	28.80	26.33	13.00	7.98	7.40	0.00	
Torque $Te=R_w*(Ws_1-Ws_2)$, $R_w=0.150Mt$	N.m	8.85	5.56	4.32	3.95	1.95	1.20	1.11	0.00	
Inlet Head, H (meters)=P/rg	m	14.26	14.26	14.26	14.26	14.26	14.26	14.26	14.26	14.26
Experimental Power, Pe = Tω	Watt	0.00	178.19	221.70	270.14	192.59	122.85	116.25	0.00	
Theoretical Power, Pt=(mw) Co^2 k(1-k)(1-cosβ2)	Watt	0.00	396.58	530.72	584.09	527.03	505.75	492.93	464.51	42.07
Theoretical Torque, Tt = (mw) Rw Co(1- k)(1-cos β2)	N.m	17.85	12.37	10.34	8.54	5.34	4.93	4.71	4.26	0.29
Input Power, Pin = ρ*g*Q*H	Watt	680.50	680.50	680.50	680.50	680.50	680.50	680.50	680.50	680.50
Experimental Overall efficiency,	$\eta_o = P_e/P_{in}$	0.00	0.26	0.33	0.40	0.28	0.18	0.17	0.00	
Bucket Speed, m/s	Co= ωr	0.00	3.40	5.44	7.25	10.47	10.88	11.10	11.55	15.54
Speed ratio, k	k =U/C0	0.00	0.21	0.34	0.46	0.66	0.69	0.70	0.73	0.98
Theoretical Hydraulic efficiency, η_{hy} =2*k*(1-k)*(1-cosβ)		0.00	0.57	0.77	0.85	0.77	0.74	0.72	0.68	0.07
Theoretical Overall efficiency, $\eta_{tO} = \eta_{hy}*0.60$		0.00	0.37	0.50	0.55	0.50	0.48	0.47	0.44	0.04

Table 4.4: Measured and calculated parameters at 25% Spear Valve Open Position

Parameters		Trial						
		1	2	3	4	5	6	7
Sppe, N	rpm	0	310	555	660	850	955	1410
Pressure, P	N/m^2	145	145	145	145	145	145	145
Volume Flow Rate, Q litres/sec (measured using Calibration of v-notch)	L/s	2.30	2.30	2.30	2.30	2.30	2.30	2.30
Angular Speed, ω	rad/sec	0.00	32.47	58.13	69.12	89.02	100.02	147.67
Net spring balance, reading (Ws1-Ws2)	N	28.00	20.73	13.47	13.00	7.07	0.00	
Torque $Te=R_w*(Ws_1-Ws_2)$, $R_w=0.150Mt$	N.m	4.20	3.11	2.02	1.95	1.06	0.00	
Inlet Head, H (meters)=P/rg	m	14.77	14.77	14.77	14.77	14.77	14.77	14.77
Experimental Power, Pe = Tω	Watt	0.00	100.97	117.42	134.79	94.36	0.00	
Theoretical Power, Pt=(mw) ̇Co^2 k(1-k)(1-cosβ2)	Watt	0.00	167.41	233.92	244.64	236.91	217.65	10.90
Theoretical Torque, Tt = (mw) ̇Rw Co(1- k)(1-cos β2)	N.m	7.00	5.16	4.02	3.54	2.66	2.18	0.07
Input Power, Pin = ρ*g*Q*H	Watt	333.26	333.26	333.26	333.26	333.26	333.26	333.26
Experimental Overall efficiency,	$\eta_o = P_e/P_{in}$	0.00	0.30	0.35	0.40	0.28	0.00	
Bucket Speed, m/s	Co= ωr	0.00	3.44	6.16	7.33	9.44	10.60	15.65
Speed ratio, k	k =U/C0	0.00	0.22	0.39	0.46	0.59	0.67	0.99
Theoretical Hydraulic efficiency, η_{hy} =2*k*(1-k)*(1-cosβ)		0.00	0.58	0.81	0.85	0.82	0.76	0.04
Theoretical Overall efficiency, $\eta_{tO} = \eta_{hy}*0.60$		0.00	0.38	0.53	0.55	0.53	0.49	0.03

Chapter Five

Result Discussions, Conclusion and Recommendation

This chapter discusses about the results conducted in the experiment making speed and flow rate constants and no load test were carried out. Thereby, validation of experimental test results with theoretical and simulation results were conducted.

4.1 Result Discussions

5.1.1 No Load Test

In this section, no load result of the manufactured micro Pelton turbine at 13.34-meter head is presented as shown in Figure 5.1.

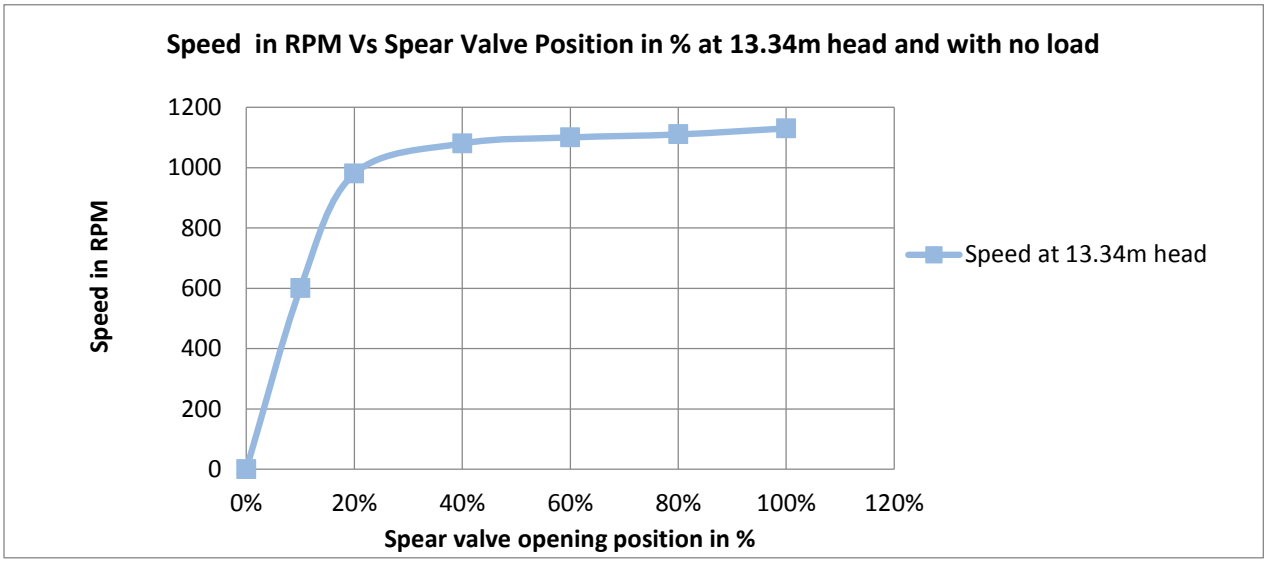

Figure 5.1: Speed Vs Spear valve open position in percentage with no load.

From the no load test, it was seen that as the valve opens more, flow rate increases and thus the increased momentum results in increasing speed of the turbine and this is within acceptable range though the runaway speed is lower than the theoretical designed due to friction losses.

More so, from visual inspection and from the speed increment range, the position of nozzle, the distance between spear valve tip to bucket, the alignment of spear valve are as per the design and the dynamic balance of the turbine was acceptable. Therefore, the turbine is ready for load test.

5.1.2 Load Test

5.1.2.1 Main Characteristic or Constant Head Curves of Pelton Turbine

Main Characteristics curves were drawn at 100%, 75%, 50% and 25 % open spear valve position at constant flow rate as charted in fig 5.2, 5.3, 5.4 and 5.5 respectively.

Relatively, the 7.8 Lit/sec flow rate will give a higher efficiency followed by the 10.41, 5.2 and 2.3 lit/sec. this is because at full open vibration increases resulting in decrease in efficiency.

From the four main characteristic curves, it can be seen that Maximum efficiency of the manufactured turbine occurs at the same speed irrespective of percent of spear valve opening as expected.

From the torque vs. speed graphs, we can see that the speed decrease proportionally with increasing torque and relatively, the 10.41 lit/sec flow rates will have more force to move the wheel thus will have the highest speed compared to the 7.8 lit/s and 5.2 lit/s flows.

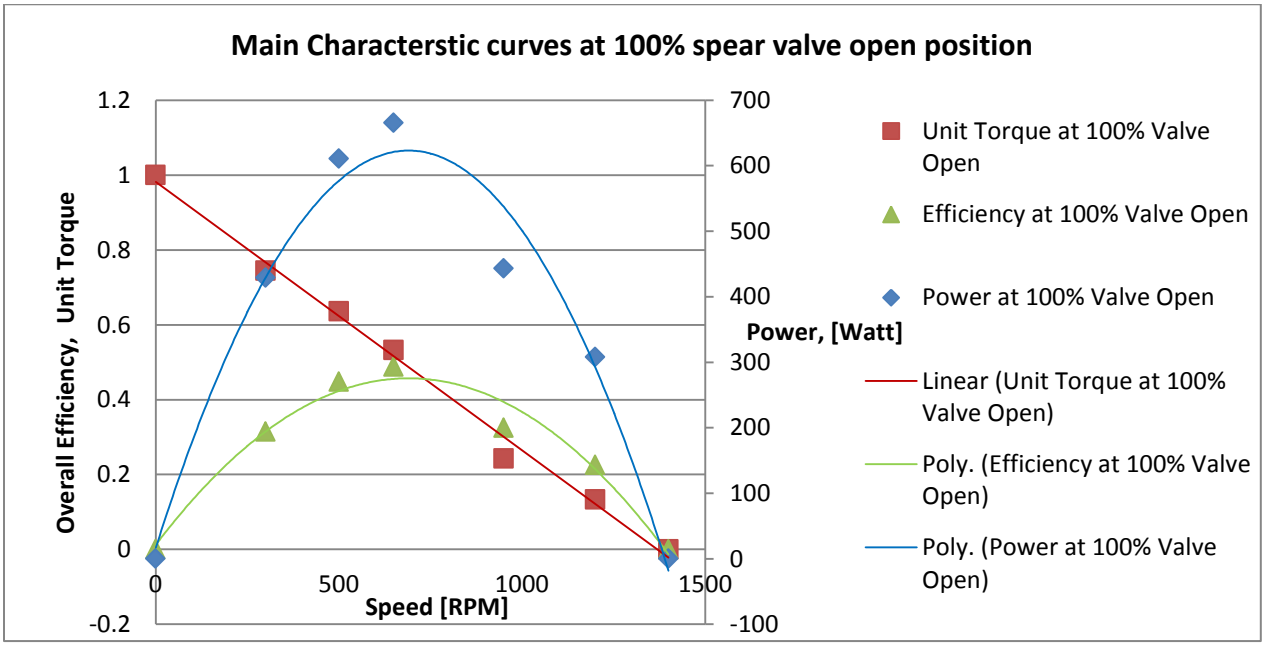

Figure 5.2: Main Characteristic Curves at 100% spear valve open position.

Power, Unit Torque and Overall Efficiency Vs Speed in RPM

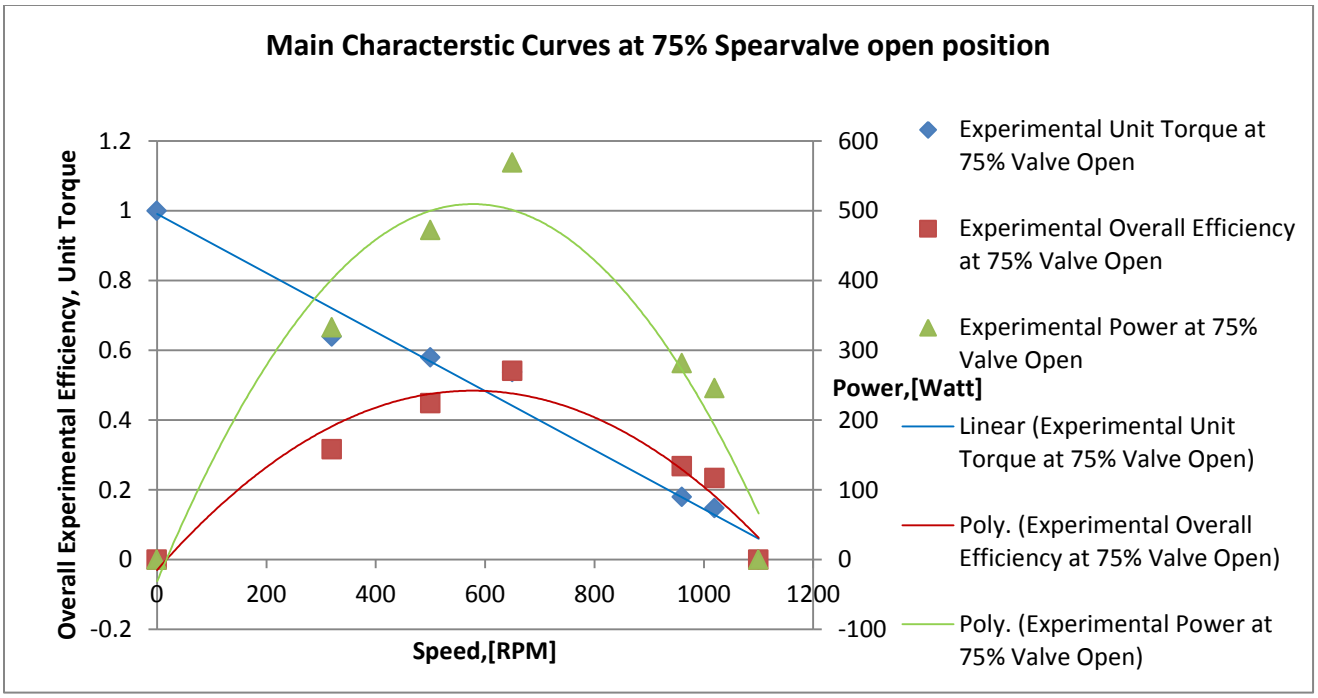

Figure 5.3: Main/Constant Head Characteristic Curves at 75% spear valve open position.

Power, Unit Torque and Efficiency Vs Speed in RPM

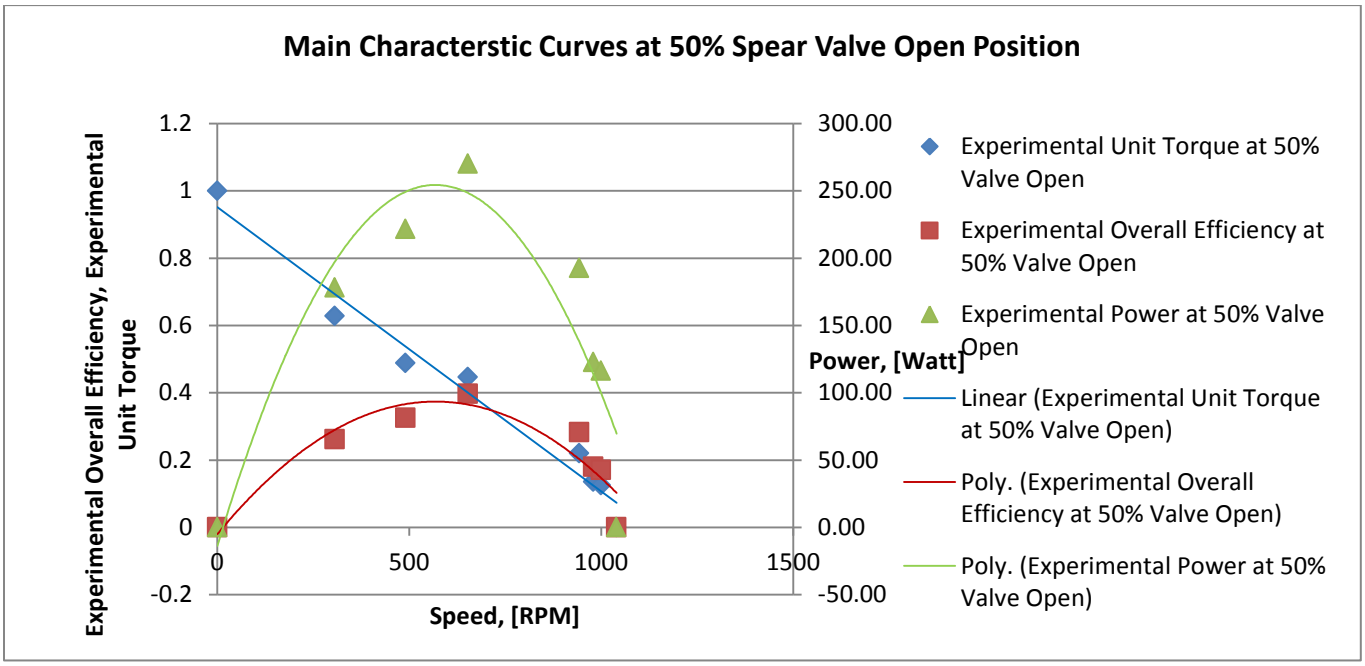

Figure 5.4: Main/Constant Head Characteristic Curves at 50% spear valve open position.

Power, Unit Torque and Efficiency Vs Speed in RPM

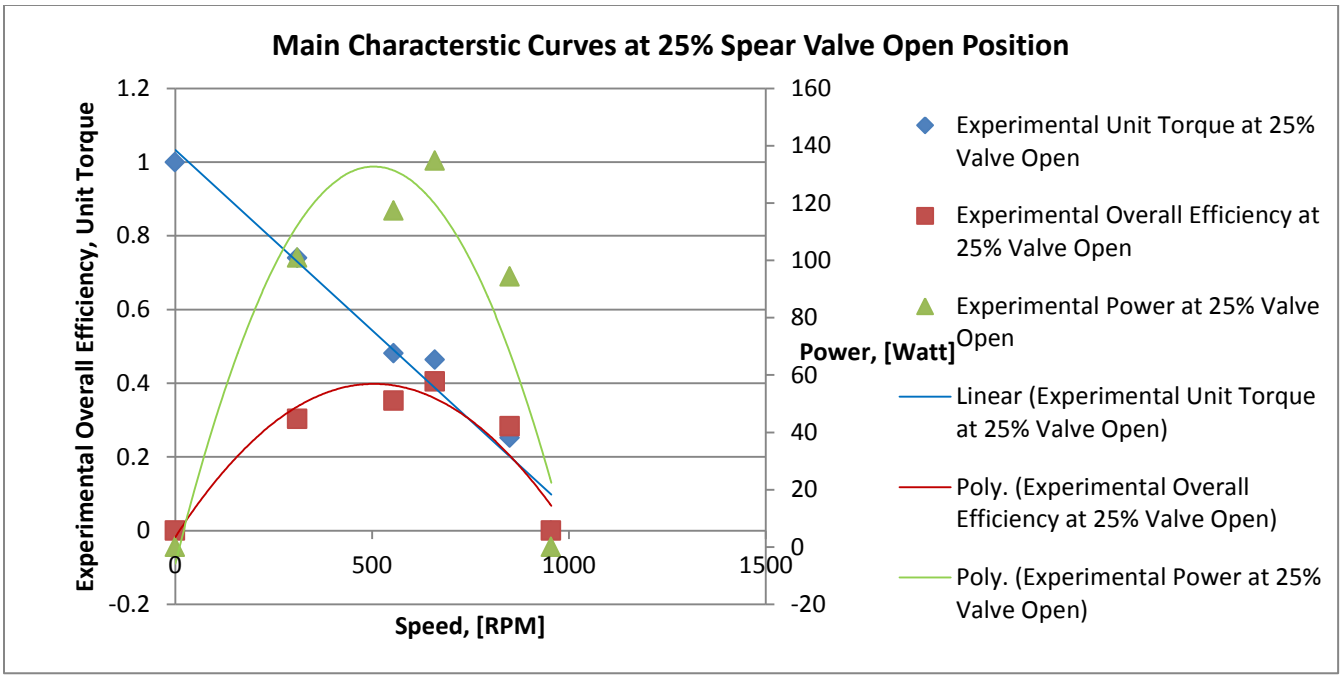

Figure 5.5: Main/Constant Head Characteristic Curves at 25% spear valve open position.

Power, Unit Torque and Efficiency Vs Speed in RPM

From Fig 5.6 below, it can be observed that maximum power could be obtained from the maximum flow rate, which is 10.41 lit/s at designed speed by keeping the head constant and the lowest power is obtained from the lowest flow rate 2.3 lit/s as expected.

Again, from Fig 5.6 it can be seen that the maximum speed at which the power curve reaches zero is less at low speed and gets higher as speed of the turbine increase and reaches nearly at run-away speed at maximum speed, this is due to high vibration loss and due to high inertial load for low speeds.

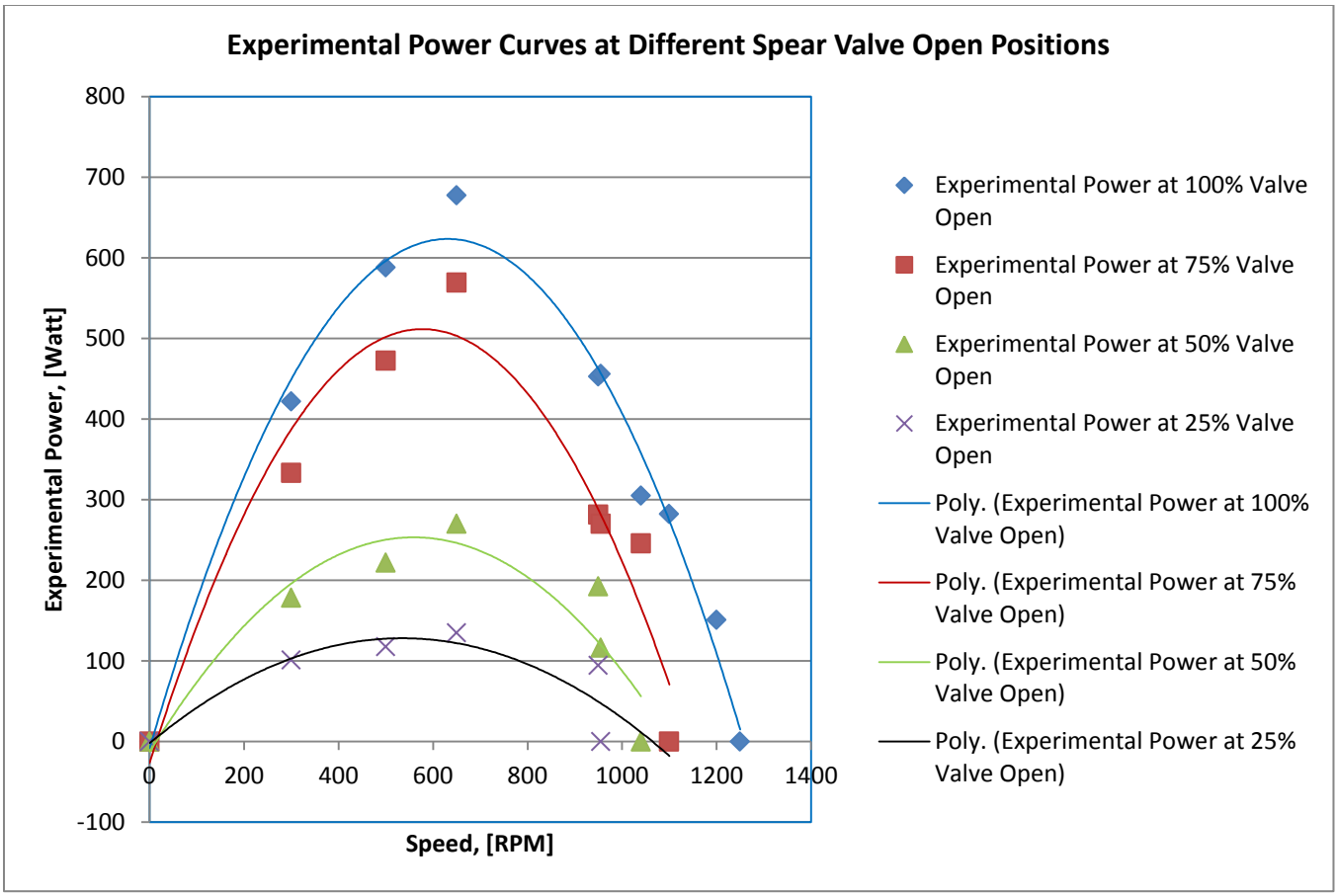

Figure 5.6: Characteristic Power Curves at different spear valve opening positions, Power Vs speed

Again, Experimental efficiency comparisons were shown in Fig 5.7 below, maximum efficiency is gained at 75% valve opening, and all the efficiency curvatures were in good alignment with expected theoretical curvatures.

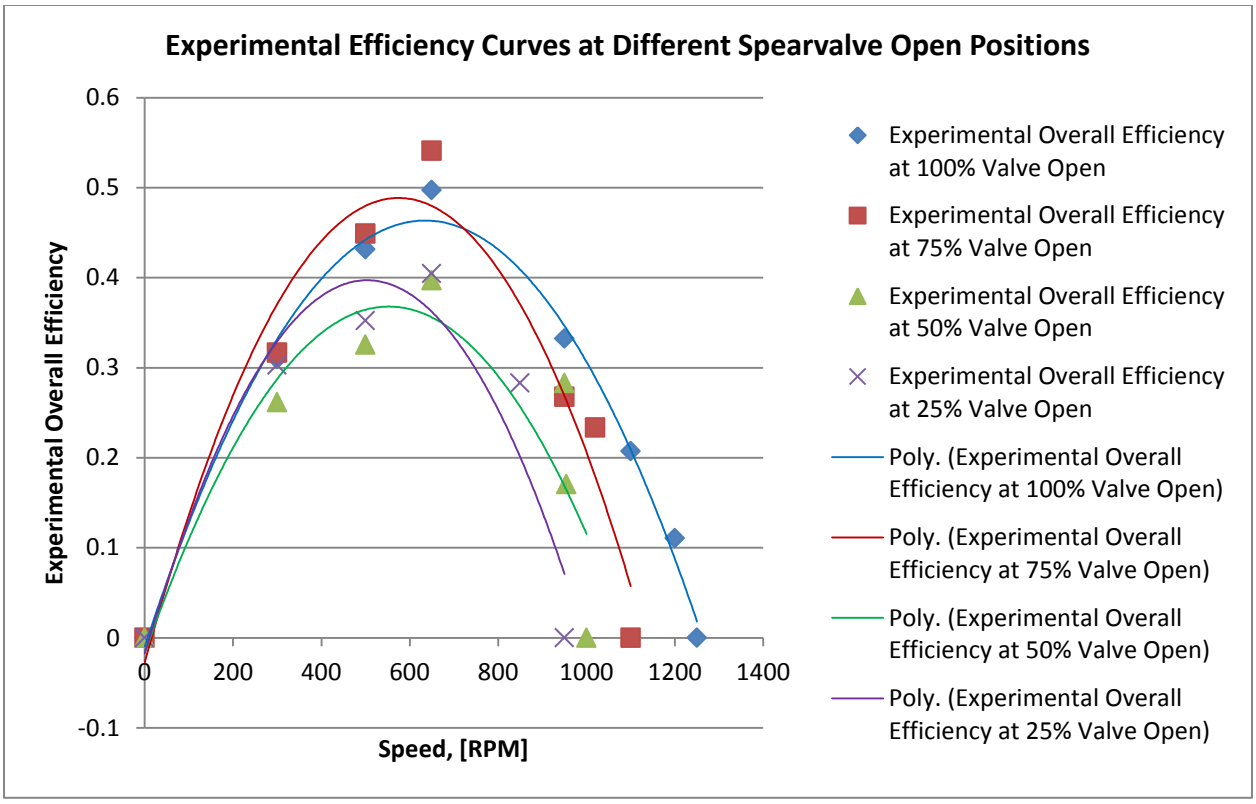

Figure 5.7: Characteristic Efficiency Curves at different spear valve opening positions, Efficiency Vs speed

5.1.2.2 Operating Characteristic or Constant Speed Curves of Pelton Turbine

Characteristics power and efficiency curves were drawn at 100%, 75%, 50%, and 25 % open spear valve position at constant speed as followed in fig 5.8 and 5.9, respectively.

From Figures5.7 and 5.8 both efficiency and power increases as the speed increases for all flow rates until the turbine reaches its designed speed. Then after design speed both parameters; power and efficiency, declines as speed increases which is as expected ass theoretical curves for Pelton Turbines.

Again, from Figures 5.7 the amount of power decreases as flow rate decreases for every specified speed, this is similar with theoretical performance curves. The curves al low RPMs is not smooth as compared with at high speeds and this is due to high vibration at low speeds.

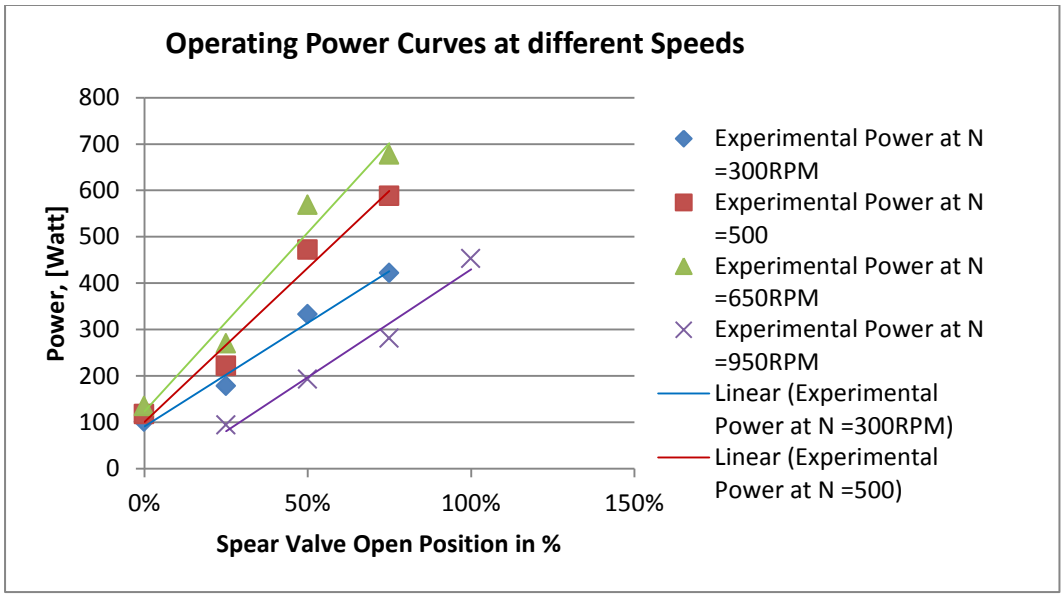

Figure 5.8: performance curve at various spear valve opening position at constant turbine speed, Power vs. spear valve opening in %

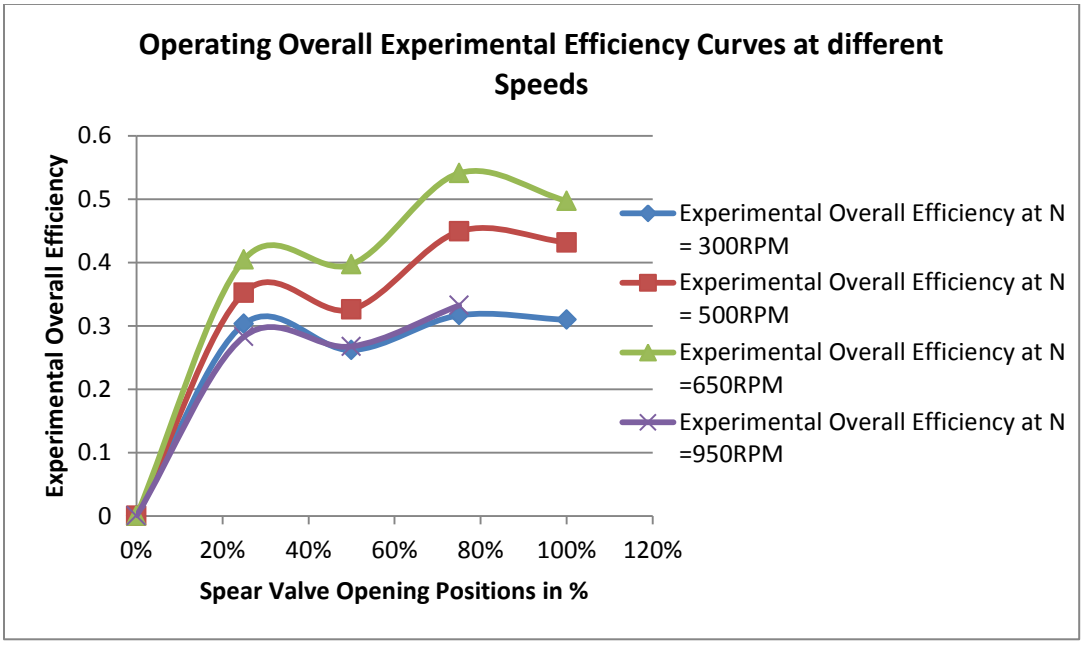

Figure 5.9: performance curve at various spear valve opening position at constant turbine speed, efficiency vs. spear valve opening in %

From Figures 5.10 the amount of efficiency increases rapidly initially until the flow rate reaches around 20% of the design flow a5nd then remain nearly constant beyond a particular value of discharge, this is similar with theoretical performance curves.

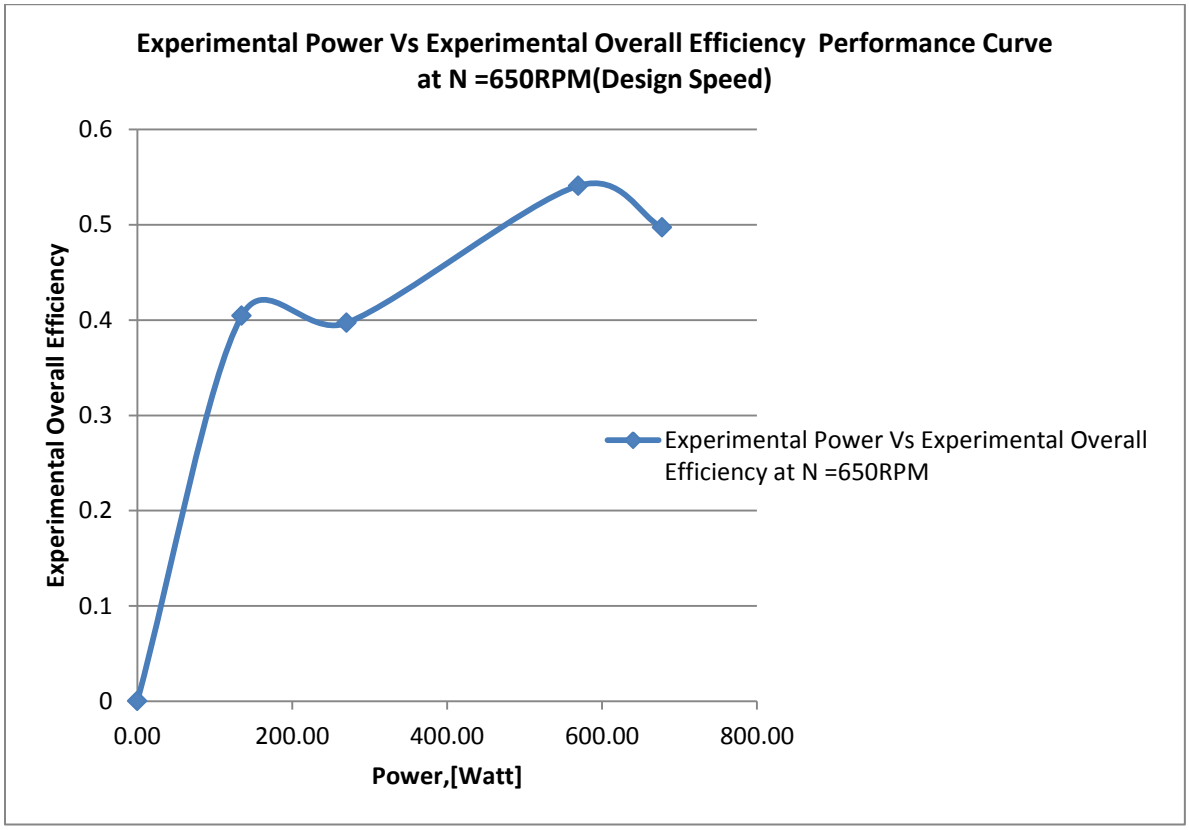

Figure 5.10: performance curve at design turbine speed, efficiency vs. power

In Fig 5.11 below both operating curves of experimental power and efficiency vs. spear valve open position is shown. From the graph, it was seen that it is similar with the theoretical result expected.

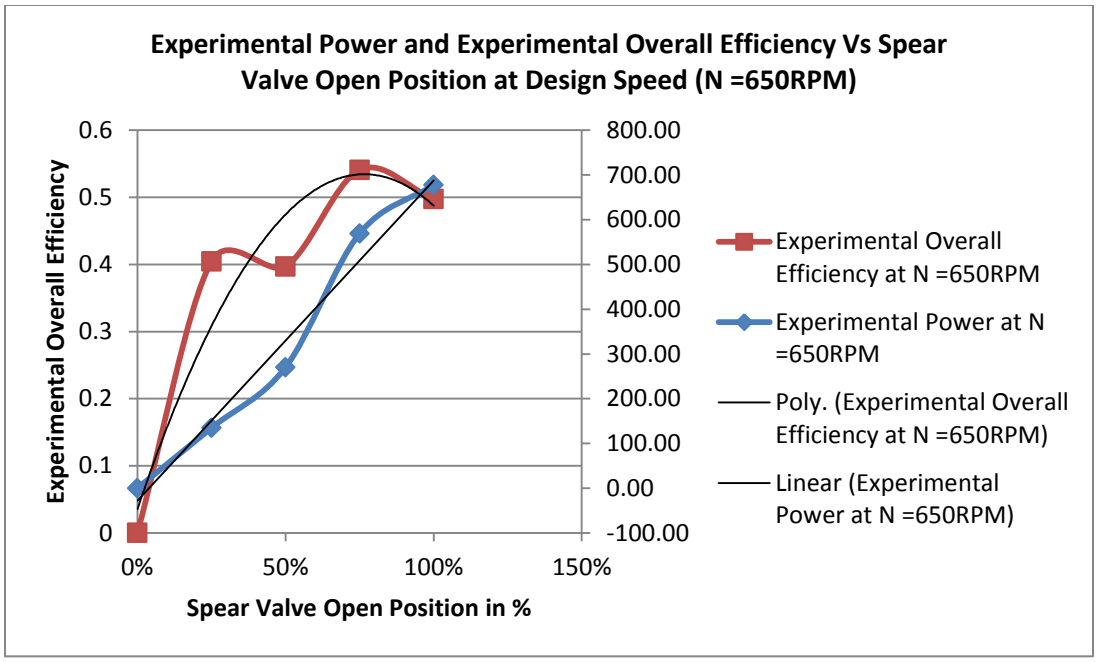

Figure 5.11: performance curve at various spear valves opening position at constant designed turbine speed of 650RPM, Power and efficiency Vs spear valve position in %.

5.2 Comparison and Validation

5.2.1 Comparison of Experimental Test and Theoretical Result

A) Constant Head Test

The theoretical hydraulic, theoretical overall (considering overall efficiency of 65%) and experimental overall efficiency are shown below in Figure. 5.12 for comparison. From Figure 5.12 the operating characteristic curve of the manufactured turbine was in line with the theoretical curve except for the value differences and the runaway speed. The runaway speed of the manufactured turbine was less than the theoretical one and this was due to frictional losses.

From the efficiency vs. speed graphs shown in Figure. 5.13, it is found that the measured efficiency is lower than the theoretical which is due to the fluid friction, which reduces the kinetic energy of the flow. As the speeds increase, the efficiency increase too until to a certain point, it will decrease meaning that the efficiency of the wheel will decrease eventually and it is impossible to reach an increasing efficiency based on the theoretical value.

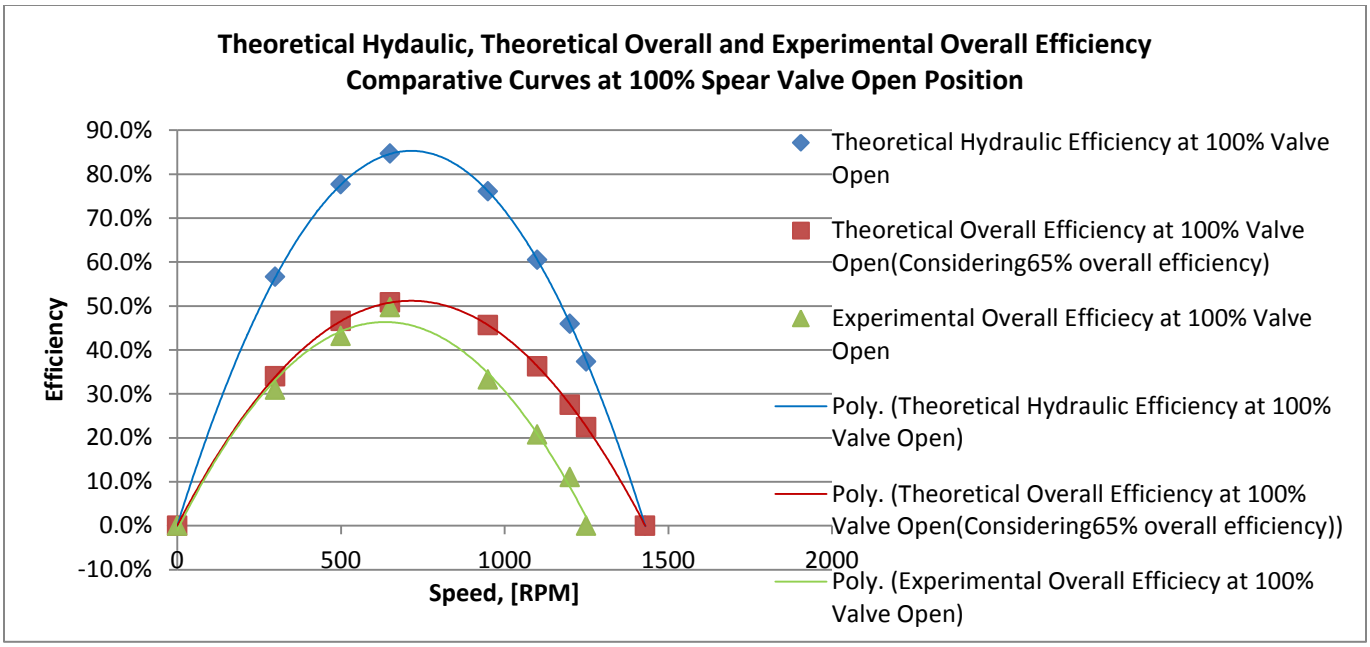

Figure 5.12: Theoretical and experimental Efficiency results Vs speed in RPM@100% valve open

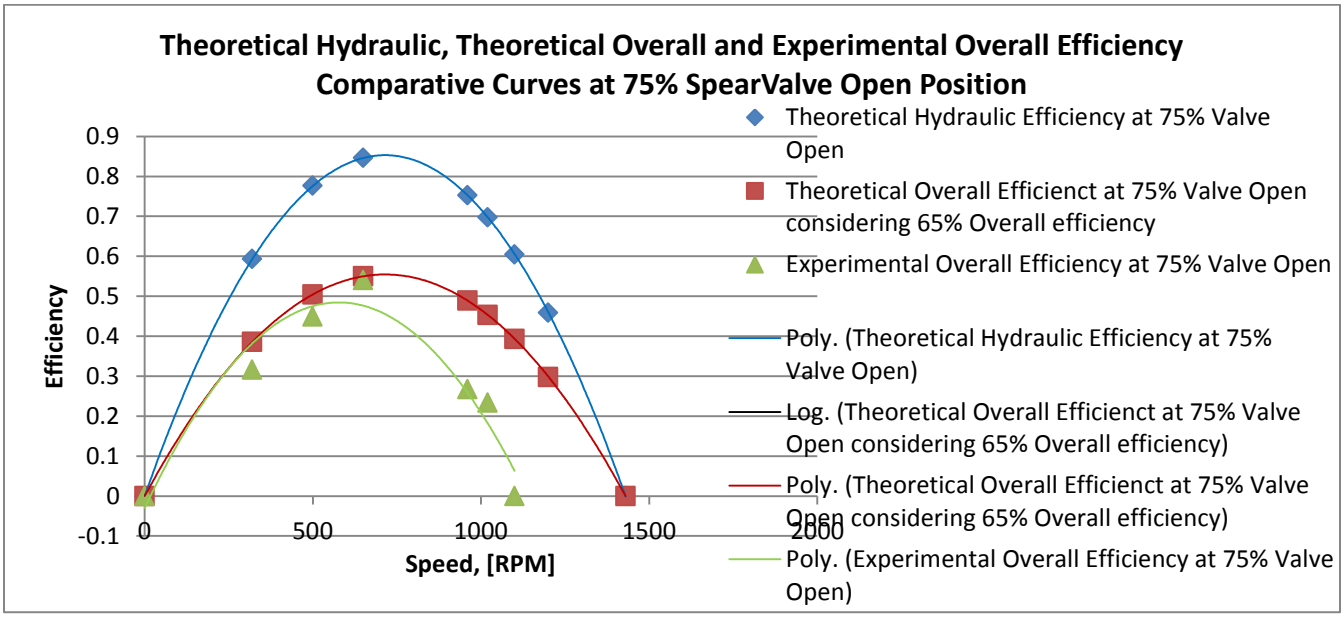

Figure 5.13: Theoretical (Hydraulic), Theoretical (Overall) and experimental (Overall) Efficiency results Vs speed in RPM @75% spear valve open

Both Experimental Power and Torque were compared with theoretical curves as in Figure 5.14, and thus from the result it is shown that the curvatures are in line with the expected performance curves.

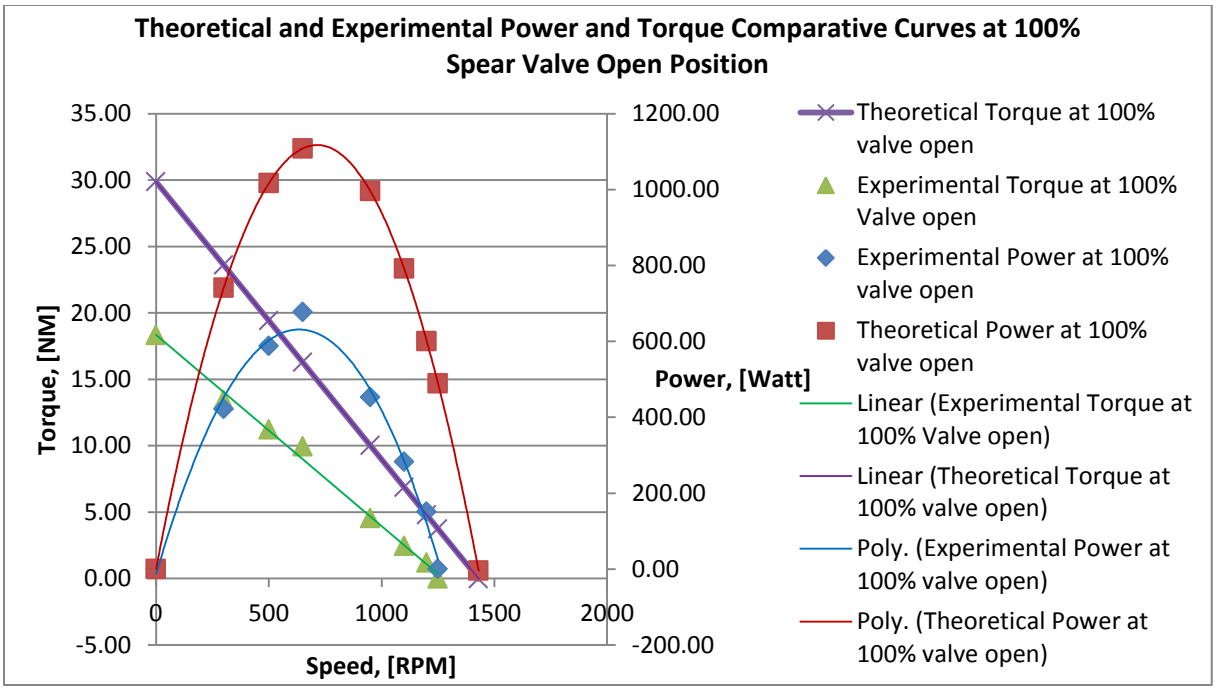

Figure 5.14: Theoretical and experimental power& Torque results Vs speed in RPM@100% valve open

The test rig in AAiT has no mechanism to measure hydraulic efficiency therefore overall efficiency is considered. The theoretical efficiency considers only hydraulic efficiency. The efficiency measured experimentally were overall efficiency, hence it was important to consider theoretical losses as per test procedures[15] and the theoretical overall efficiency expected from the manufactured turbine was 56% but the measured efficiency was 54.09% and this results in a 3.41% error at 75% valve open position and is within acceptable range.

B) Constant Speed Test

From Figure 5.15 it was seen that the shape of characteristic curve of the turbine at constant speed were similar with expected curve shape. The power curve increases linearly as the spear valve opens more i.e. power increase as flow rate increases and this is as expected with theoretical. The runaway speed of the experimental result was less than the theoretical and this is due to friction losses and efficiency of the manufactured buckets.

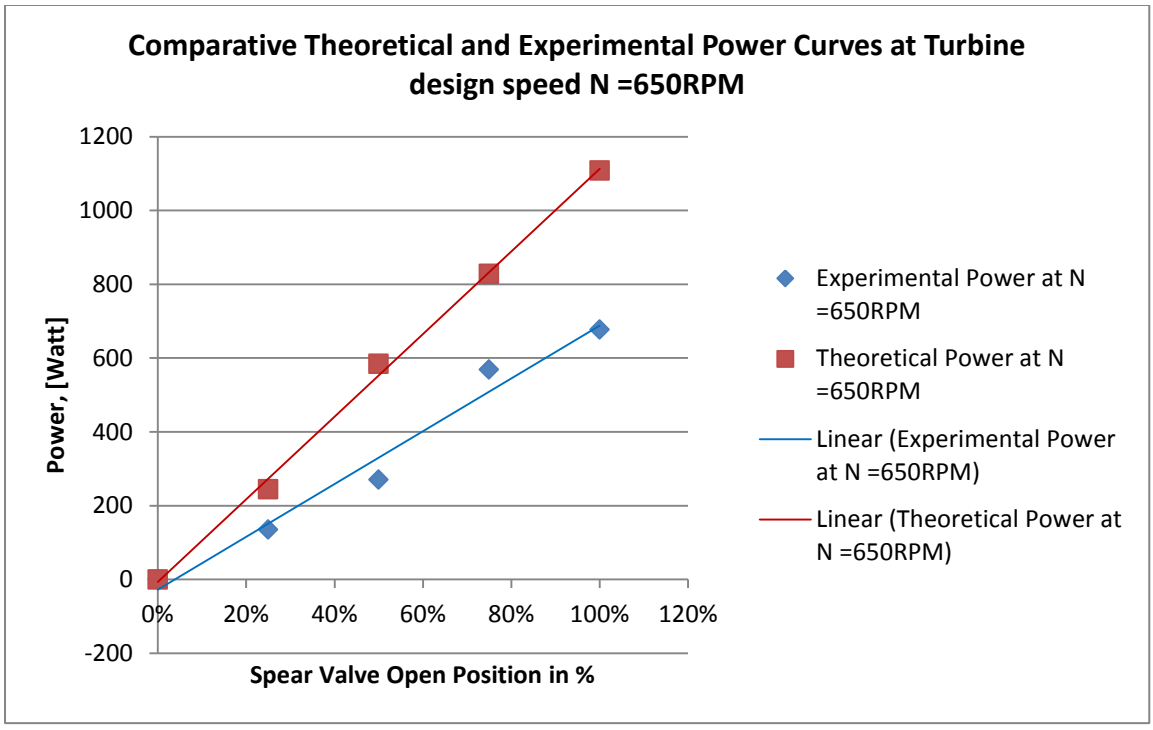

Figure 5.15: comparative curve of theoretical and experimental power at constant speed N= 650RPM at varying spear valve opening positions in %, power Vs spear valve open position in %

In Figure 5.16 below comparative efficiency curves are shown and it can be seen that the experimental overall efficiency curvature is similar with both hydraulic and theoretical overall efficiency curvatures. In all cases, the efficiency curves increases at fast rate initially till it reaches around 30% of design flow to reach at turbine's runaway speed and becomes asymptotically constant and a further flow increment is not resulting in turbine speed and efficiency increased as expected theoretically.

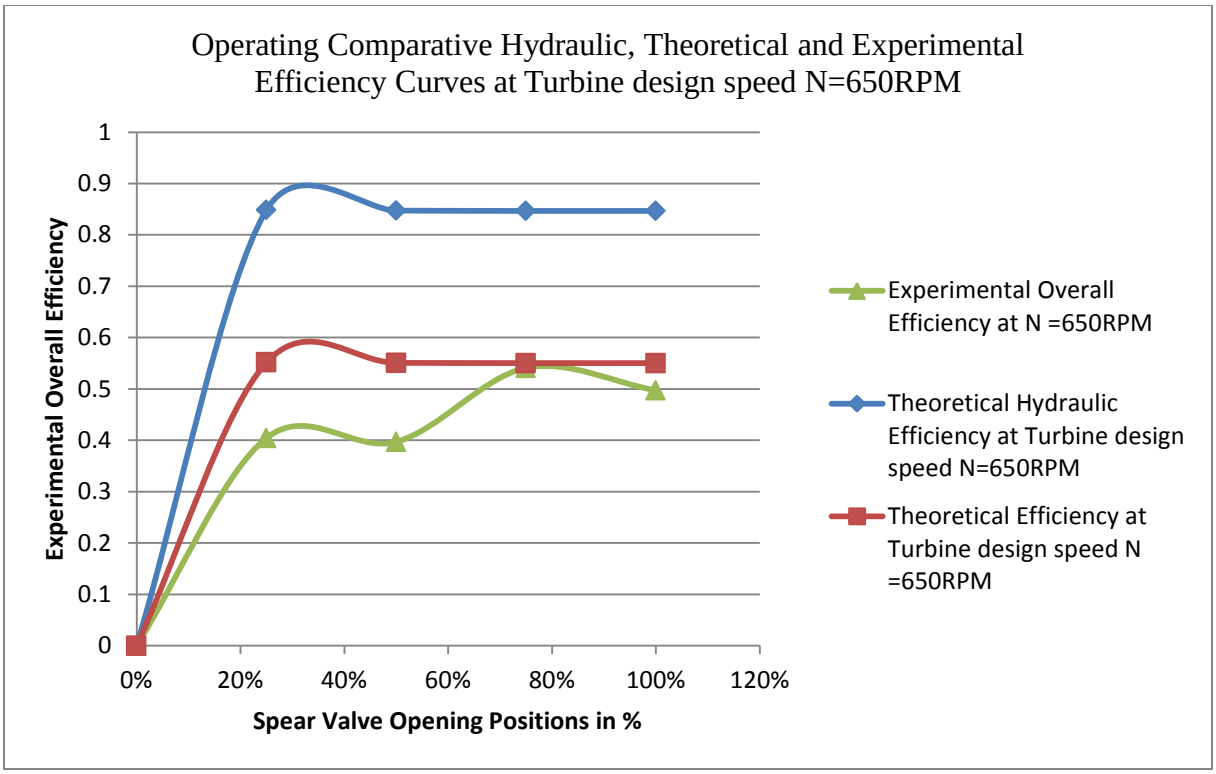

Figure 5.16: comparative curve of theoretical and experimental efficiency at constant design speed N= 650RPM at varying spear valve opening positions in %.

5.2.2 Comparison of simulation and Experimental Test Result

Only single jet operation was modeled assuming that increasing the efficiency in single jet operation would increase the performance with both jets in operation as well. Therefore, a comparison of numerical and experimental results was performed at this operating point using the single jet results. To compare the CFD simulation results to the experimental data, different sources of the hydraulic and mechanical losses were taken into consideration. Losses that were present in the experimental testing but were not modeled are bearing friction losses, disc friction losses, injector losses, water interference due to the casing and mechanical losses (bearing, brake pad, disc friction and Nozzle losses).

Numerically predicted efficiency was over predicting as expected compared to the values measured experimentally at full nozzle open [Fig 5.17]. Considering the lack of local experiences and right machines and tools for manufacturing of Pelton turbine, the reduction of efficiency is within the expected error range.

Again, it was expected that CFD results would over predict the efficiency since the splashing and water interference effect caused by the casing was not included in the CFD model. Comparison of Theoretical and experimental results were shown and from Figure 5.17 it was seen that the turbine has a good performance starting from 25% of design flow.

The CFD simulation result has shown the turbine performs good starting from 20% the designed flow. From both comparisons the turbine was manufactured excellently and the manufacturing procedures followed was correct and can be scaled up for mass productions using this work as fabrication manual.

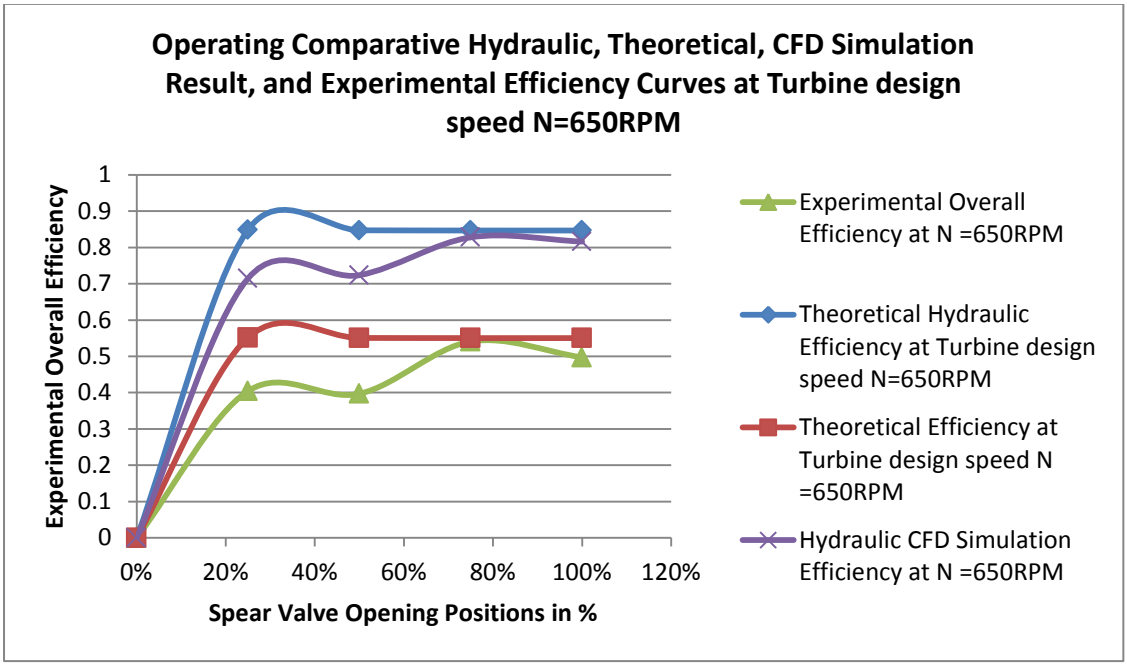

Figure 5.17: Theoretical Hydraulic, Theoretical Overall, CFD Simulation and Experimental Efficiencies Vs spear valve open position in% at design Turbine constant speed N=650RPM.

5.3 Conclusion and Recommendation

5.3.1 Conclusion

In this study, a model of Pelton turbine has been manufactured and experimentally tested in AAiT Hydraulics laboratory. The first stage was to perform a literature search on the existing manufacturing information. It was found that there is no of local fabrication experience available.

Manufacturing of bucket was done using sand casting using the 3D printed bucket as master pattern. This method was good to obtain the acceptable efficiency of the turbine and hence the method can be scaled up.

Manufacturing methods and procedures were developed to fabricate other parts of the turbine which plays a significant role in gaining a good efficiency and hence the procedures can be used as a manufacturing manual for micro/small turbines fabrications.

The manufactured turbine has an overall efficiency of 54.09%, which is 3.41% less from the expected theoretical overall efficiency at 75% valve opening, and the error obtained is within acceptable range. Hence, the manufacturing procedure followed was correct and can be scaled up.

The turbine has a good offload performance as compared to the CFD simulation result that shows the manufactured turbine has a good performance curve.

The variation between theoretical and experimental test result and simulation with experimental test result was occurred due to quality of manufacturing (especially casting of bucket) and inconvenience test rig at AAiT.

5.3.2 Recommendation

This experimental study forms a foundation for localization of turbines. From the manufacturing process manufacturing of buckets were difficult as there is no experience in the country hence further manufacturing technology and methods should be studied for casting of Pelton buckets.

Reference

1. Azeb Asnake, C. E. (October 21st 2015). THE ETHIOPIAN ENERGY SECTOR – INVESTMENT OPPORTUNITIES. *UK-ETHIOPIA TRADE & INVESTMENT FORUM 2015* (pp. 1-24). LONDON, UK: ETHIOPIAN ELECTRIC POWER.

2. Shanko, M. (December 2009). *Target Market Analysis Ethiopia's Small Hydro Energy Market.* GTZ

3. Bolon, W., Sharma, V., & Singh, M. (March 16, 2010). *GREEN MECHATRONICS PROJECT:PELTON WHEEL DRIVEN MICRO-HYDRO PLANT.* Ottawa: University of Ottawa.

4. Tilahun, A. (May 2011). *ASSESSMENT OF MICRO HYDRO POWER POTENTIAL OF SELECTED ETHIOPIAN RIVERS- A CASE STUDY IN THE NORTHWEST PART OF THE COUNTRY.* Addis Ababa: Addis Ababa Institute of Technology, School of Graduate Studies, Addis Ababa University.

5. www.Stratasys.com, 3D printing machine manufacturers.

6. www.engineeringtoolbox.com data sheet for Mechanical properties of aluminum.

7. Quinox.org. (1st September 2013). *Design and Construction of a 10KW Pelton Turbine, , Project Code: 0578.*Rwanda.

8. www.mrt-castings.co.uk for Casting tolerances of different materials.

9.Thake, J. (2001). *The Micro-Hydro Pelton Turbine Manual:Desighn,Manufacture and Installation For Small Scale Hydro-Power.* London,United Kingdom: ITDG Publishing.

10. Veselý, J., & Varner, M. (n.d.).*A Case Study of Upgrading of 62.5MW Pelton Turbine.* Czech Republic: ČKD Blansko Engineering.

11. Subbarao, P. P. (2008-2009). *Nozzeles and Jets for Pelton Wheels.* Delhi: Indian Institute of Thechnology Press.

12.A Group of Laboratory Staff at University of Techn. (September 14,2014). *Script of Fluid Machineries.* Iraq: Republic of Iraq Ministry of Higher Education and Scientific Research.

13. Koirala, R., Chitrakar, S., Maharjan, N., Gurung, N., & Aryal, B. P. (September 2014). Design and Development of a Reversible Pump Turbine Test Rig. *Rentech Symposium Compendium, Volume 4* (pp. 80-85). Nepal: Kathmandu University.

14. Židonis, A., & Aggidis, G. A. (2015).*Pelton Turbine: Identifying the Optimum Number of Buckets Using CFD.* Lancaster: Lancaster University Renewable Energy Group and Fluid Machinery Group, Engineering Department.

15.COMESA284. (2007). *Hydraulic turbines, storage pumps and pump-turbines –Model acceptance tests.* IEC publications.

16. Zh.Zhang. (2016). *Pelton Turbines.* Zurich: Springer International Publishing Switzerland .

17. Gudukeya, L. K., & Mbohwa, C. (2013). Improving the Efficiency of Pelton Wheel and Cross-Flow Micro Hydro Power Plants. *World Academy of Science, Engineering and Technology 83* , 1047-1061.

18. Takagi, M., YoshinobuWatanabe, Ikematsu, S., Hayashi, T., Fujimoto, T., & Shimatani, Y. (January1,2014). 3D-Printed Pelton Turbine: How To Produce Effective Technology linked with Global Knowledge. *Energy Producing*, 1593-1596.

19. Saif Aldeen Saad Obayes and Mohammed Abdul KhaliqQasim. (June 2017). Effect of Flow Parameters on Pelton Turbine Performance by Using Different Nozzles. *International Journal of Modeling and Optimization,Vol. 7, No. 3*, 128-133.

20.Barstad, L. F. (2012, June 10). *CFD Analysis of a Pelton Turbine.* Norwegian University of Science and Technology,Department of Energy and Process Engineering.

21.Y. BEUCHER, E. B. (July 12-15,2010). CHARACTERIZATION OF FRICTION LOSS IN PELTON TURBINE. *International Refrigeration and Air Conditioning Conference*, (pp. 2274, Page1-8). Purdue.

22.Chukwuneke J. L., Achebe, C. H., Okolie, P. C., & Okwudibe, H. A. (2014). Experimental Investigation on Effect of Head and Bucket Splitter. *Journal of Information Engineering and Applications Vol.4, No.10*, 48-54.

23.Bryan, R. C., & Kendra, V. S. (2012, september 20). Impulse (Turgo and Pelton) turbine performance characteristics and their impact. *Renewable Energy 50(2013)*, pp. 959-964.

24. Olaoye, J. O., & Oyebode, O. (November 2014). Design and Fabrication of Pelton Wheel and Cross Flow Turbines for Power Generation. *Proceedings of the International Soil Tillage Research Organisation (ISTRO) Nigeria Symposium* (pp. 101 – 109). Akure: Department of Agricultural and Biosystems Engineering,University of Ilorin, Ilorin, Kwara State, Nigeria.

25.Eisenring, M. (Septembe1991). *Micro Pelton Turbines* . Niederuzwi, Switzerland: SKAT, Swiss Center for Appropriate Technology.

26. William , A., & Simpson, R. (November 2008). Pico Hydro-Reducing Thechnical Risks for Rural Electrification. *ISESCO Science and Technology Vision*, 60-66.

27. .www. NationFacts.net

28.SÖKMEN, A. P., & DEMİRCİ, R. A. (2016). *Pelton Turbine Test Experimental Sheet.* BURSA TECHNICAL UNIVERSITY.

29. Thake, J. (2001). *The Micro-Hydro Pelton Turbine Manual:Desighn,Manufacture and Installation For Small Scale Hydro-Power.* London,United Kingdom: ITDG Publishing.

Appendixes

Appendix A: SOLIDWORKS Manufacturing Drawings of PeltonTurbine Parts

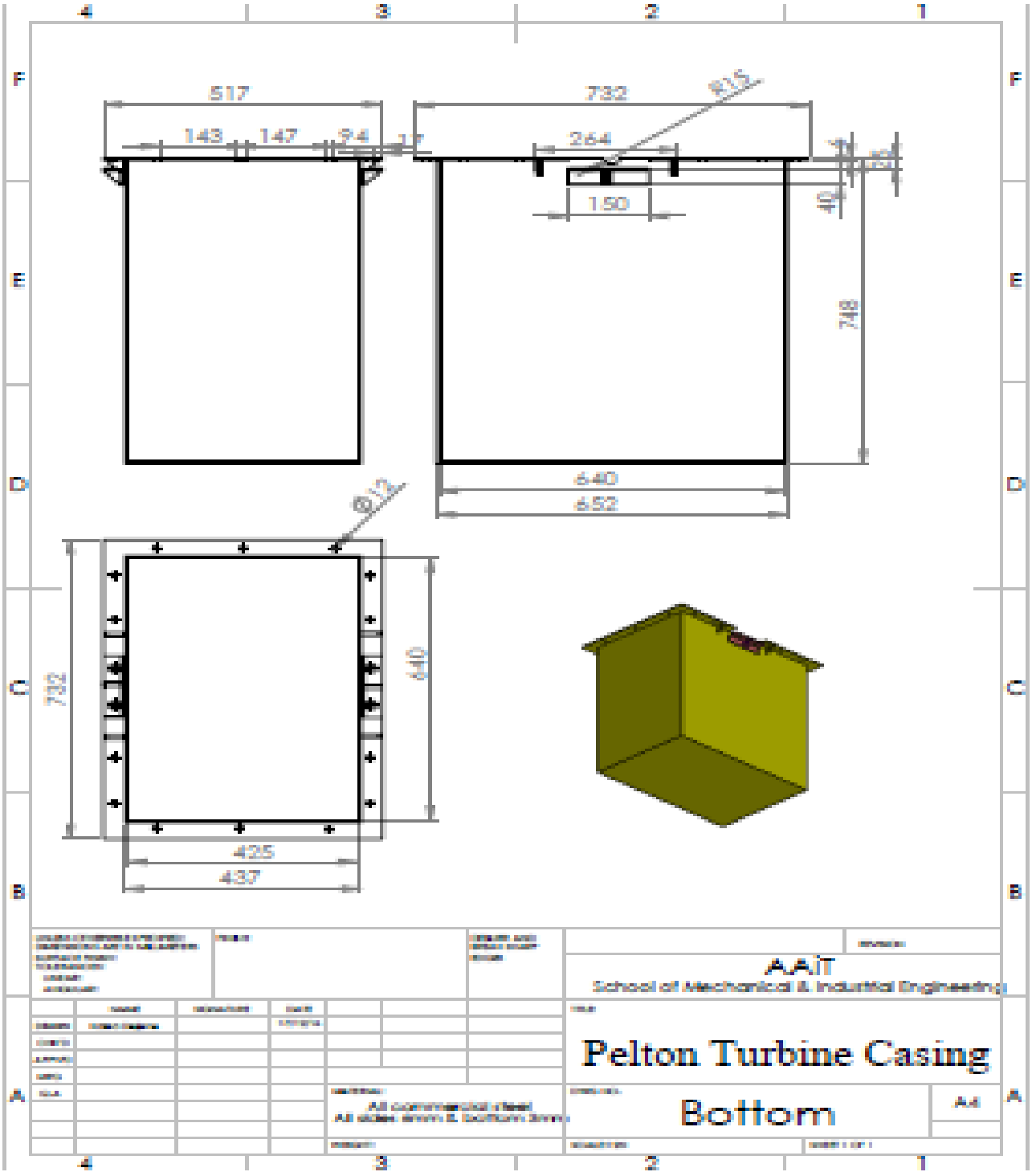

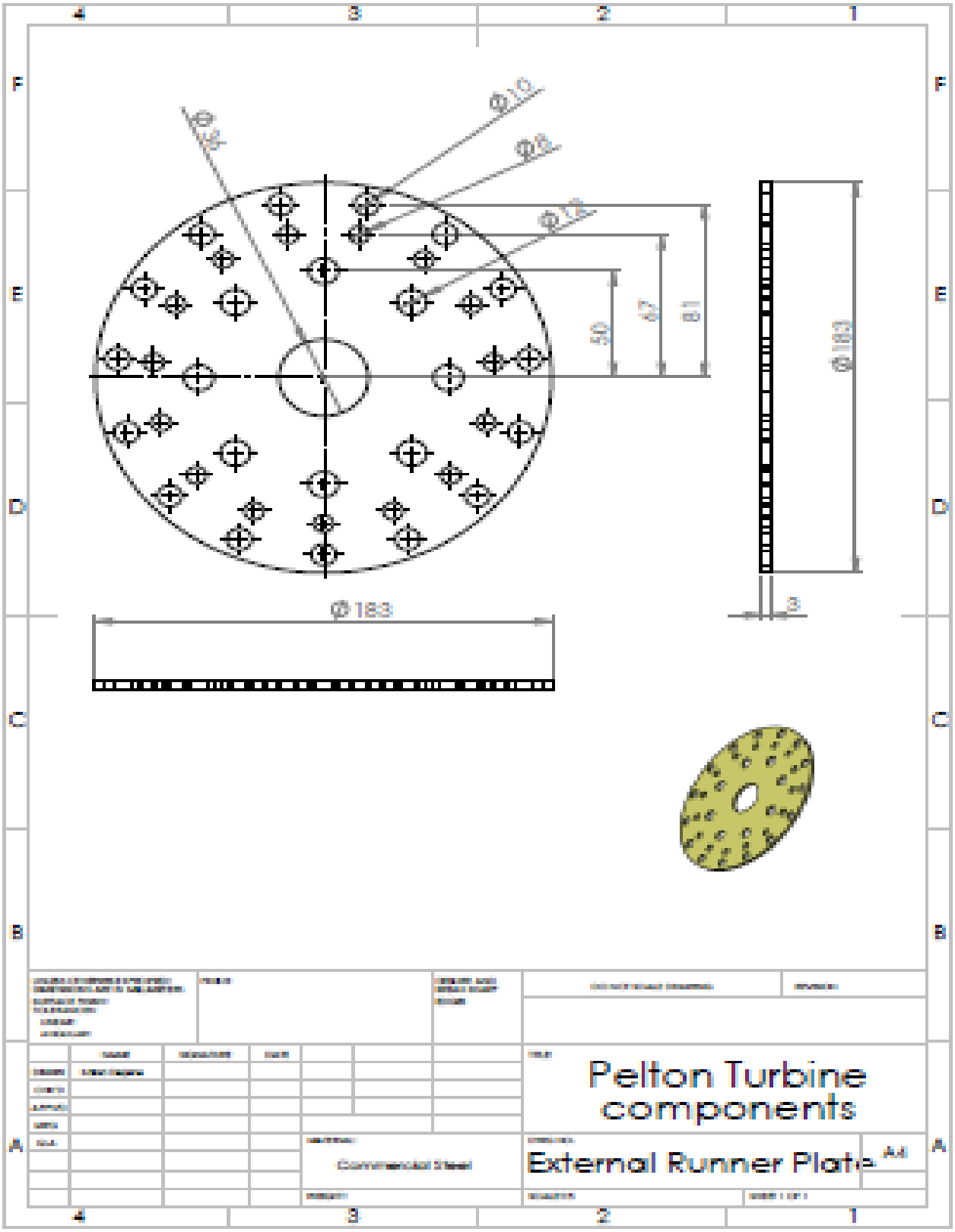
Ø10
Ø8
Ø12
50
67
81
Ø183
3
Ø183
Pelton Turbine components
External Runner Plate
Commercial Steel
A4

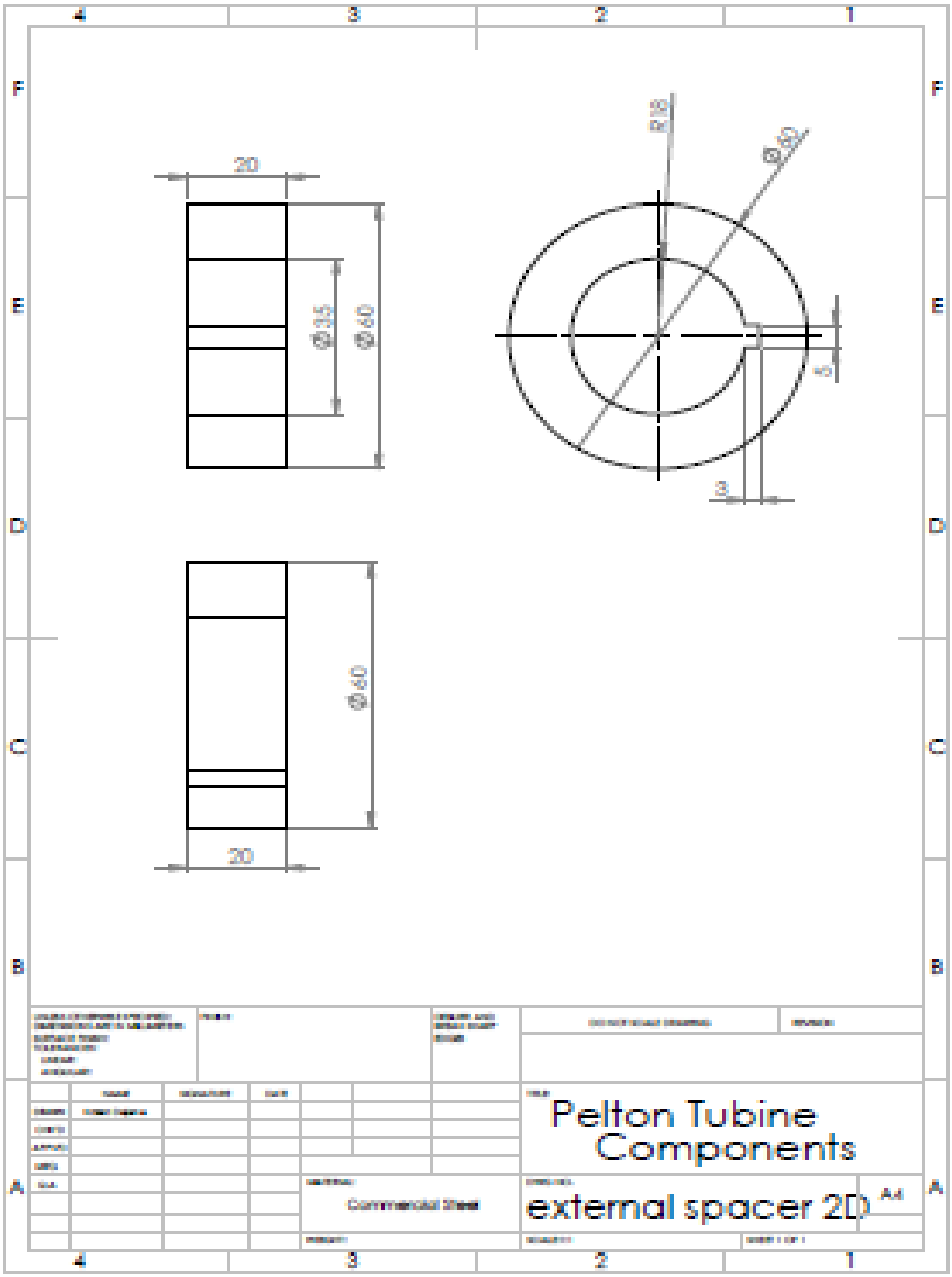
20
Ø35
Ø40
R18
Ø80
5
3
Ø40
20
Pelton Tubine Components
external spacer 2D
A4
Commercial Steel

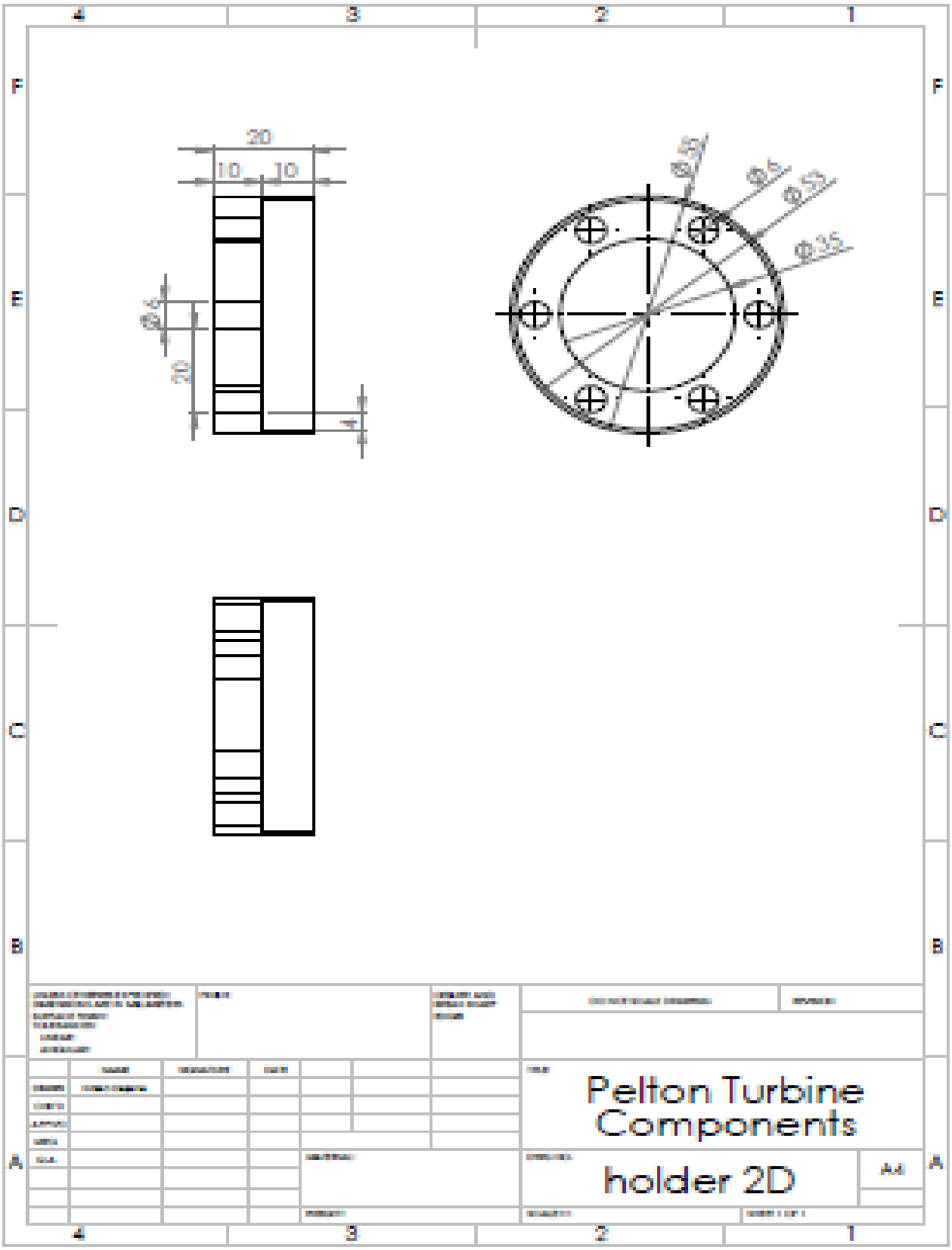
20
10
10
Φ6
30
4
Φ57
Φ6
Φ53
Φ35
Pelton Turbine Components
holder 2D
A4

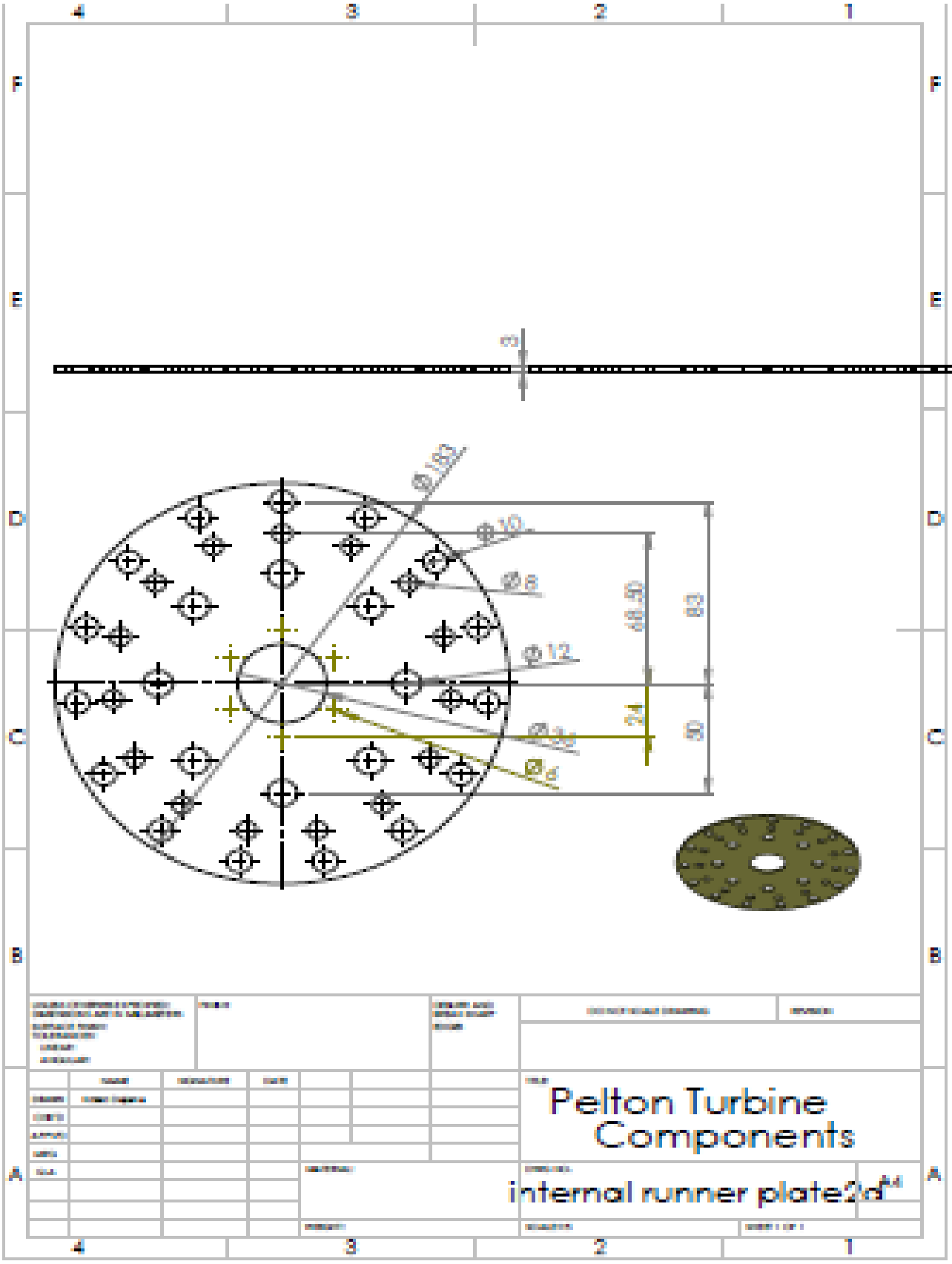
Pelton Turbine
Components
internal runner plate2d

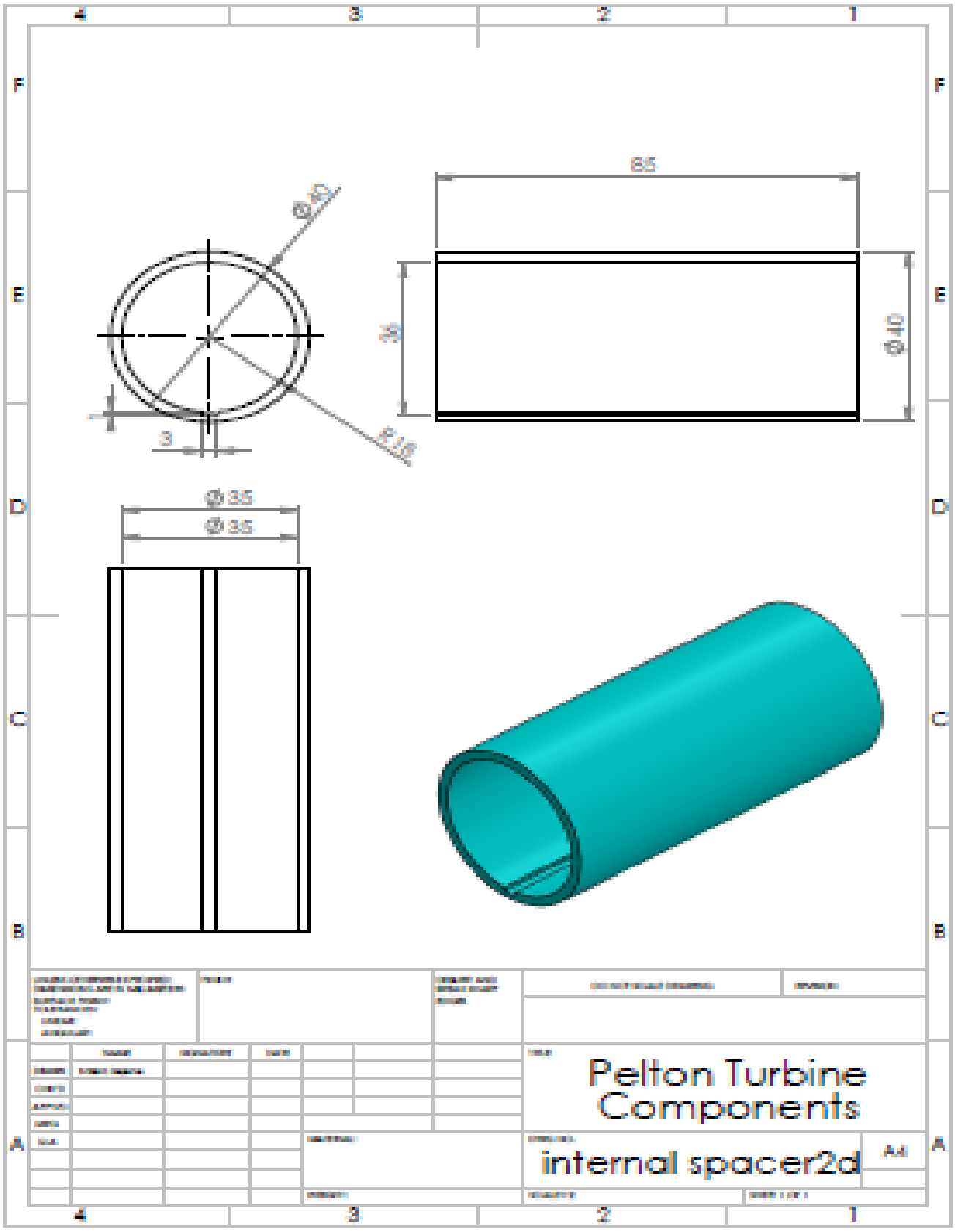
4
3
2
1
F
E
D
C
B
A
85
Ø40
36
Ø40
3
R18
Ø35
Ø35
Pelton Turbine Components
internal spacer2d
A4

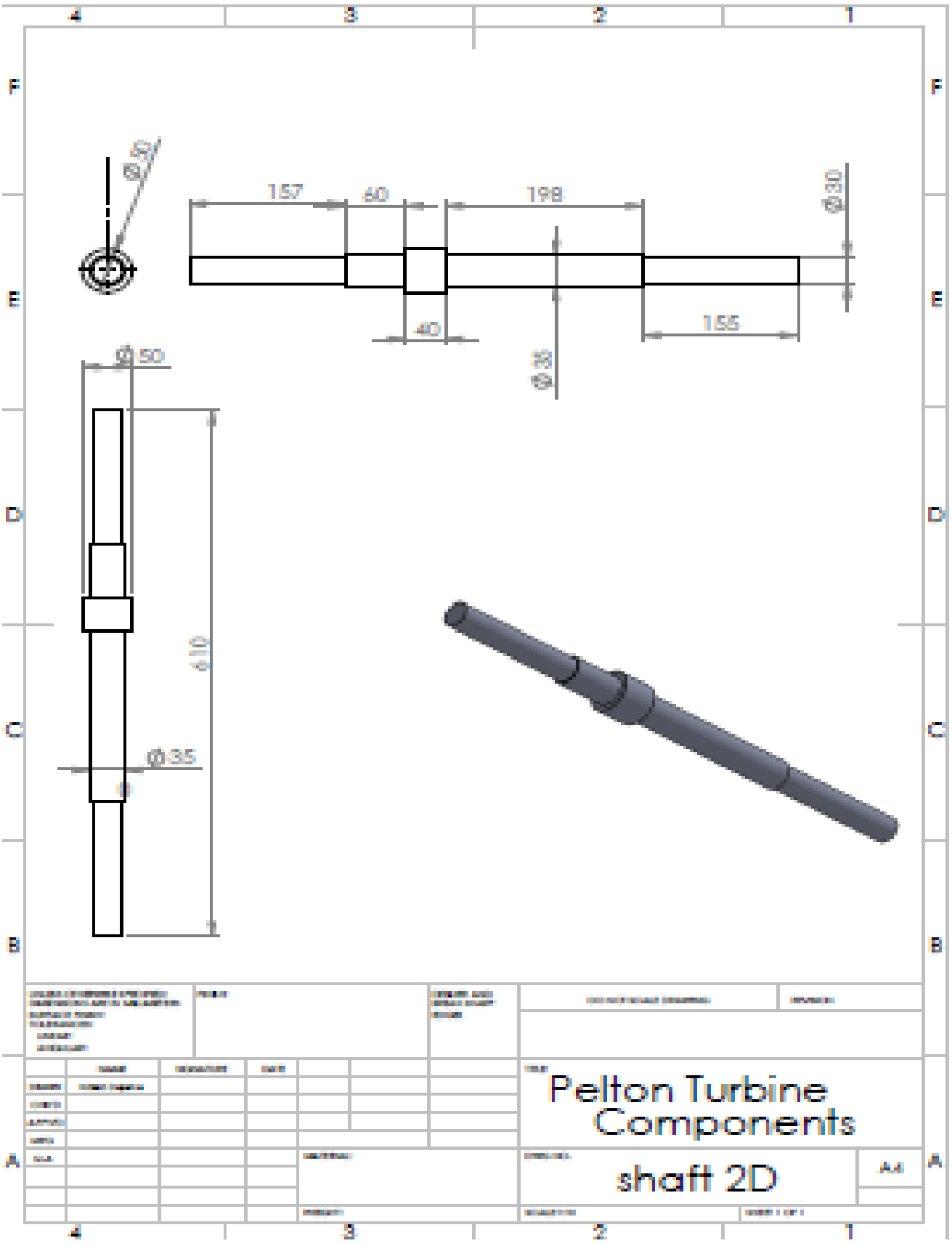
157
60
198
Ø30
40
155
Ø50
410
Ø35
Pelton Turbine Components
shaft 2D
A4

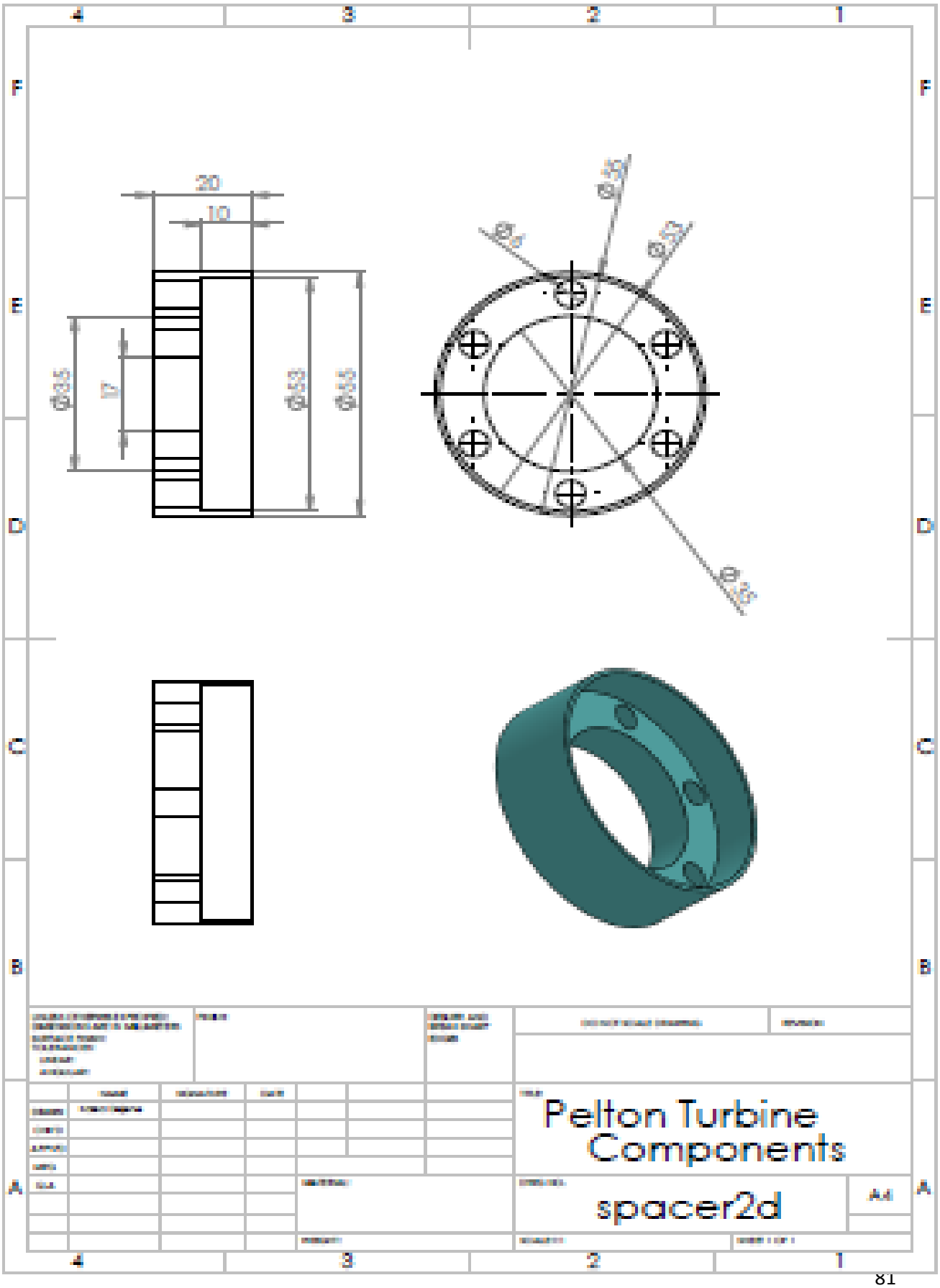
20
10
Ø35
17
Ø53
Ø35
Ø39
Ø53
Ø47
Pelton Turbine Components
spacer2d
A4

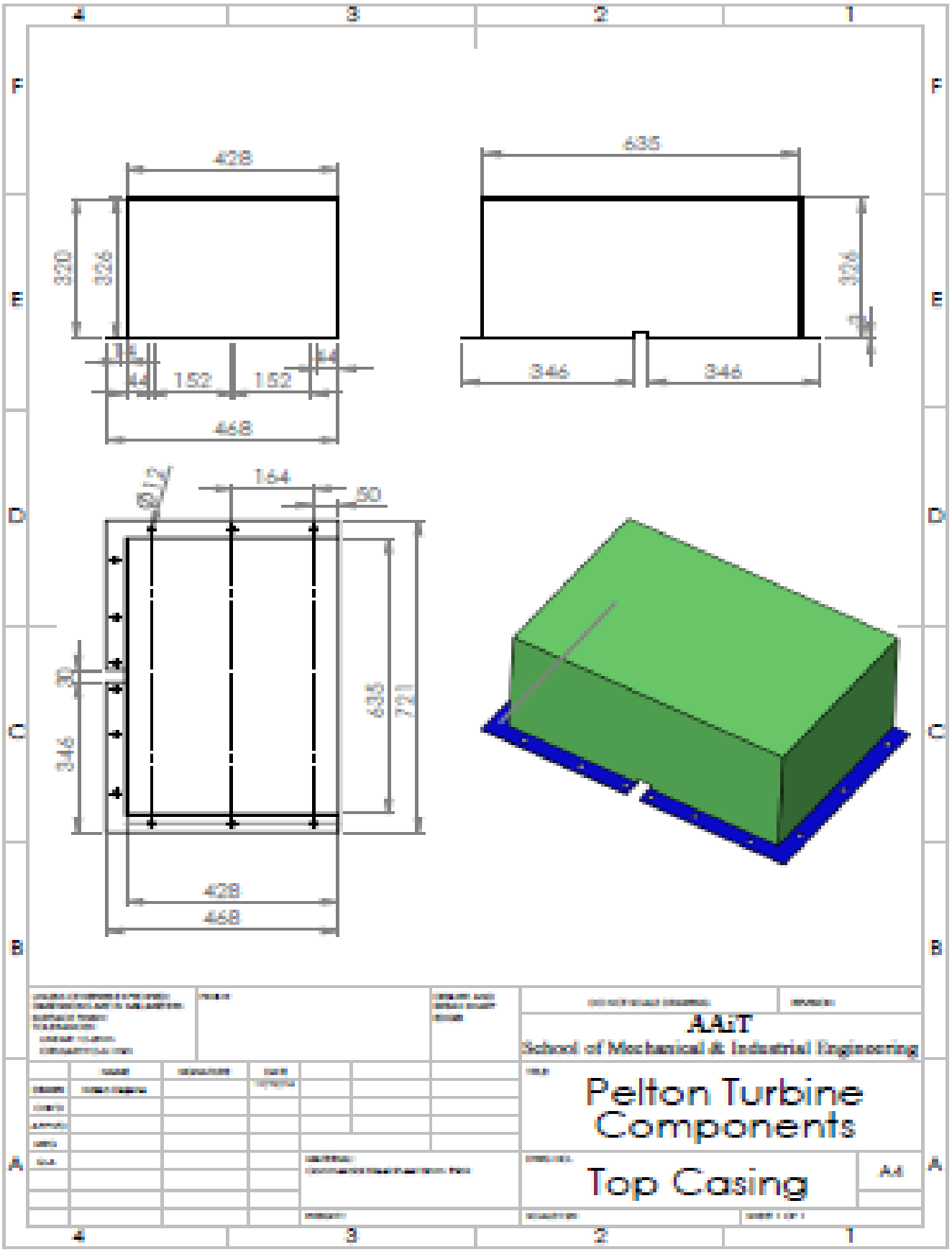
428
320
326
44
152
152
44
468
635
326
346
346
12
164
50
30
346
635
721
428
468
AAiT
School of Mechanical & Industrial Engineering
Pelton Turbine Components
Top Casing
A4

Annex B: Calibration procedure of V-notch Height measure

Name of Student: Test Date: Group: CALIBRATION OF V-NOTCH

Calculation Sheet Page 6

	Value	Dim	1	2	3	4	5	6	7	8	9	10	11
①	water level h'	mm											
②	$h = h' - h_o$, $h_o = 954.7$ mm	mm											
③	$\Delta p_{orifice}$ (=12.55 Δp_{or}. mmHg)	mmWc											
④	$\Delta p_{orifice} = 9.81 \cdot ③$	$\frac{kg}{m.s^2}$											
⑤	$\frac{2}{\rho}\Delta p_{orifice} = \frac{2}{\rho} \cdot ④$	$\frac{m^2}{s^2}$											
⑥	$\sqrt{\frac{2}{\rho}\Delta p_{orifice}} =$ ⑤	$\frac{m}{s}$											
⑦	$\frac{V}{\alpha} = A_d\sqrt{\frac{2}{\rho}\Delta p_{orifice}} = A_d \cdot ⑥$ $A_d = 3.142 \times 10^{-3}$	$\frac{m^3}{s}10^{-3}$											
⑧	$\alpha_{Orifice} = f(V/\alpha)$ see graph	1											
⑨	$V = (V/\alpha).\alpha = ⑦ \cdot ⑧$ Orifice Orifice	$\frac{m^3}{s}$											

Page 7

⑩	$\sqrt{h} = ②$	$m^{1/2}$											
(11)	$h^2 = ②^2$	m^2											
(12)	$\sqrt{2gh} = 4.428 \cdot ⑩$	m/s											
(13)	$\frac{8}{15}\sqrt{2gh} \cdot h^2 = 0.5333 \cdot (12).(11)$	$\frac{m^3}{s}$											
(14)	$\alpha_{notch} = \frac{V_t}{(13)} = \frac{(9)}{(13)}$	1											
(15)	δ												
(16)													

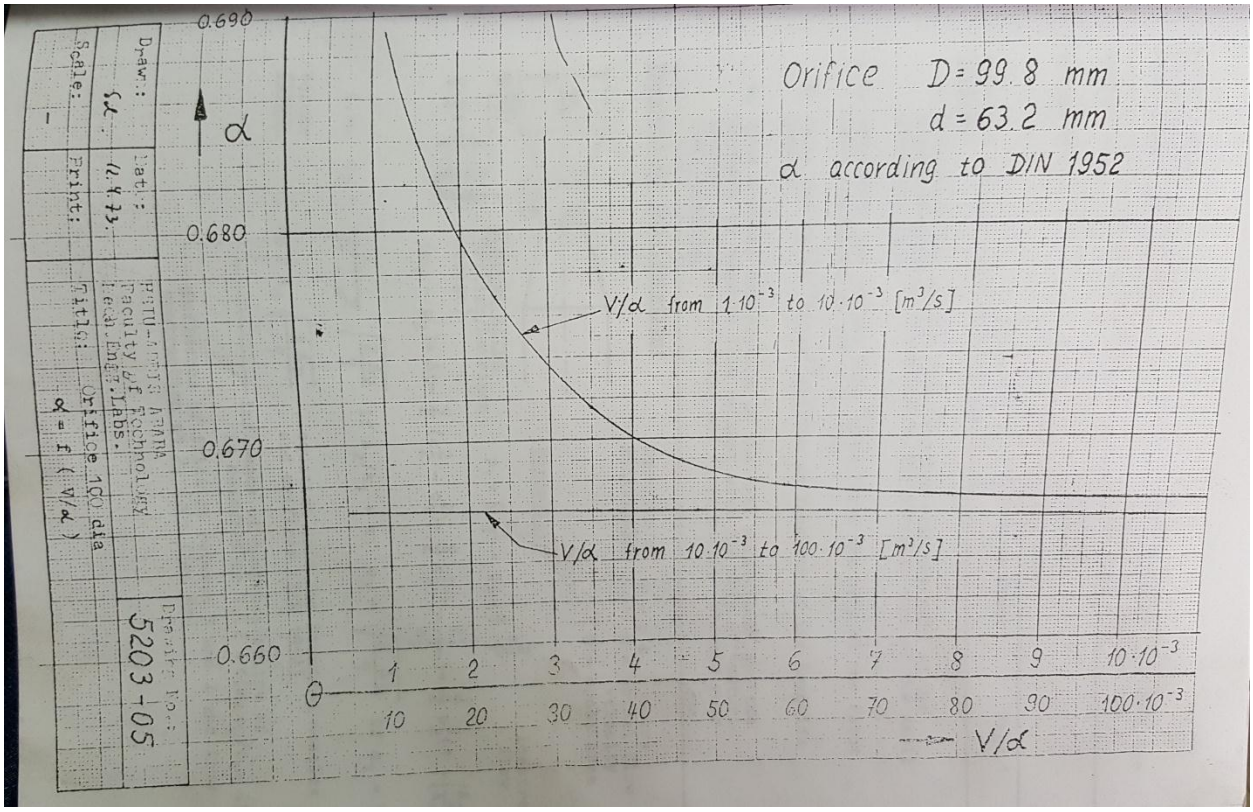

Machines Laboratory — Calibration of V-Notch — Page 5

Year: Name of Student: Group: Test Date:

			1	2	3	4	5	6	7	8	9	10
1	Δp_{orfice}	mm (Hg-wc)										
2	Δp_{orfice}	mmWc										
3	h' water level	mm										
4	h' -h_o = h' –954.7mm	mm										
5	Setting position of pelton Turbine Nozzle											
6												